



Comments on the Intermediate-Temperature Embrittlement of Metals and Alloys: The Conditions for Transgranular and Intergranular Failure

Antonio Enrique Salas-Reyes ¹, Abdullah Qaban ^{2,*} and Barrie Mintz ^{2,*}

¹ Departamento de Ingeniería Metalúrgica, Facultad de Química, UNAM, Ciudad de México 04510, Mexico; enriquesalas@comunidad.unam.mx

² Department of Mechanical Engineering and Aeronautics, City University of London, London EC1V 0HB, UK

* Correspondence: abdullah.qaban@city.ac.uk (A.Q.); barrie.mintz@city.ac.uk (B.M.)

Abstract: The intermediate-temperature embrittlement range was examined for Fe, Al, Cu, and Ni alloys. It was found that this embrittlement occurs in many alloys, although the causes are very diverse. Embrittlement can be due to fine matrix precipitation, precipitate free zones, melting of compounds at the grain boundaries, segregation of elements to the boundaries, and, additionally for steel, the presence of the soft ferrite film surrounding the harder austenite matrix. Grain boundary sliding and segregation to the boundaries seem to dominate the failure mode at the base of the trough when intergranular failure takes place. When cracking is due to the presence of hydrogen or liquid films at the boundary, then the dissociation along the boundaries is so easy, it is often independent of the strain rate and is always intergranular. In the other cases when failure occurs, if the deformation is carried out at a high strain rate, it is normally transgranular (e.g., hot rolling giving rise to edge cracking). However, when the strain rate is reduced to that of creep (e.g., bending during continuous casting of steel), failure can also take place by grain boundary sliding, and intergranular failure then becomes the favoured mode.

Keywords: hot ductility; Fe, Al, Cu, and Ni alloys; segregation; intergranular and transgranular failure; grain boundary sliding; precipitation



Citation: Salas-Reyes, A.E.; Qaban, A.; Mintz, B. Comments on the Intermediate-Temperature Embrittlement of Metals and Alloys: The Conditions for Transgranular and Intergranular Failure. *Metals* **2024**, *14*, 270. <https://doi.org/10.3390/met14030270>

Academic Editors: Xiao-Wu Li and Tomáš Prošek

Received: 14 December 2023

Revised: 17 January 2024

Accepted: 15 February 2024

Published: 24 February 2024



Copyright: © 2024 by the authors. Licensee MDPI, Basel, Switzerland. This article is an open access article distributed under the terms and conditions of the Creative Commons Attribution (CC BY) license (<https://creativecommons.org/licenses/by/4.0/>).

1. Introduction

Hot deformation of metals and alloys is very complex, involving the formation of crystal defects, the strengthening by them, temperature softening and fracture, and their flow behaviour can be quantified by the strain, strain rate, and working temperature. Usually, grain boundary embrittlement occurs by segregation of specific elements to the grain boundaries and by dynamic precipitation within the matrix and at the grain boundaries. During hot working, dynamic recovery (DRV) and or dynamic recrystallisation (DRX) take place, and this is often followed by grain growth. All these processes have to be accounted for in order to interpret the hot-ductility behaviour.

Unfortunately, many ductile metals and alloys have a ductility trough in the hot working temperature range; this is referred to as intermediate-temperature embrittlement or hot-ductility loss and is measured by the reduction in area (RA) or elongation at fracture in high-temperature tensile tests [1]. For example, when coarse-grained tensile specimens from ferrite/pearlite steels are tested at low strain rates (10^{-2} to 10^{-4} s⁻¹) in the temperature range 700 to 1000 °C after cooling from the austenite, a ductility trough often occurs in which the ductility, as measured by RA values, is excellent at the top and bottom of this temperature range but can be very poor in the middle, giving rise to intergranular failures [2]. An increase in the strain rate, refinement of the grain size, and prevention of precipitation during cooling, particularly at the austenite grain boundaries, generally lead to an improvement in ductility and a reduction in the depth of the trough [1–6]. The

information from this curve has practical importance because this poor ductility leads to cracking occurring during the unbending operation when continuous casting steels. In this case, the explanation normally given to explain the trough is that a thin film of deformation-induced ferrite forms on cooling from the austenite. The ferrite films, being softer than the austenite grains they surround, take most of the strain, leading to “ductile” intergranular failure, which is initiated by inclusions or precipitates situated along the boundaries. These ferrite films form on phase transformation, and deformation can lead them to form over a wide temperature range [1].

However, these troughs, although normally associated with steel, can be present in nonferrous alloys and their cause can be very diverse, as with steel. In this paper, the term “intermediate-temperature range” refers to a $\sim 100\text{--}200\text{ }^{\circ}\text{C}$ span, centred at a temperature approximately half of the melting point of the alloy, conditions which favour creep when strain rates are low.

The present review explores the presence of all these hot-ductility troughs and whether there is any common denominator which may link them together.

2. Hot Ductility of Steels

Considerable scientific work has been carried out in understanding the hot-ductility trough for low-carbon steels and it is only proposed to summarise the findings here, although because steel is being used as a benchmark, more detail is required when necessary [1–6]. In HSLA (high strength low alloy) steels, the depth of the trough increases with increasing grain size, finer precipitation, and decreasing strain rate and is dependent on the composition [1–3,5,6]. Grain boundary sliding (GBS) is generally an important feature in these low-ductility intergranular failures, as both the slow strain rate during the unbending operation ($10^{-3}\text{--}10^{-4}\text{ s}^{-1}$) and the temperature of deformation when straightening the strand during continuous casting are in the range for creep. As such, it is not surprising that precipitation at the boundaries, making it easier for cracks to propagate and on deformation fine precipitation occurring within the grains increasing the shear stress acting on the grain boundaries, will both encourage GBS, favouring intergranular fracture. Although increasing the volume fraction of precipitation will lead to worse ductility, the fineness of the precipitation has the overriding influence, as can be seen from Figure 1 [2]. For a given volume of precipitation, the finer this is, the worse is the hot ductility. At the grain surface, when there is a finer distribution of the precipitation, crack growth is very much encouraged as the reduced spacing between the particles makes interlinkage of the crack front much easier. Hence, slower cooling is generally recommended.

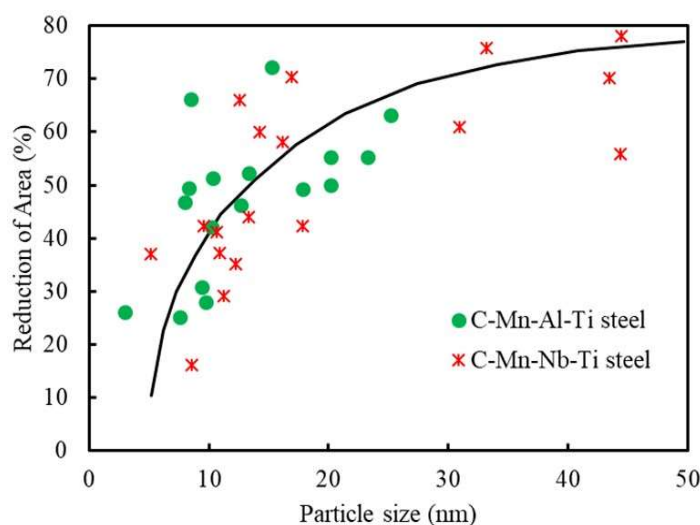


Figure 1. Influence of particle size for C-Mn-Al-Ti and C-MnNb-Al steels, adapted with permission from [2], 2010, Taylor & Francis.

Because GBS is dependent on diffusion, decreasing the strain rate will increase the time available for sliding to occur, again favouring intergranular failure. Coarser grains probably worsen the ductility (see Figure 2) by increasing the crack length along the grain boundary before the path is blocked by encroachment of the crack with an adjacent grain [1–3].

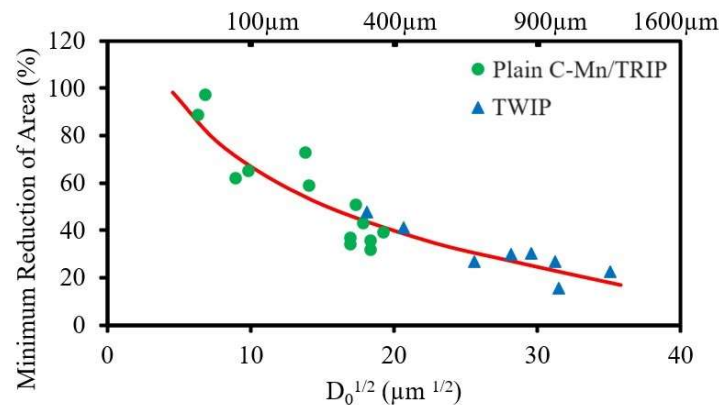


Figure 2. Influence of grain size on the RA (reduction in area) value of steels, where D_0 is the original grain size before deformation for steels having 0.15% C, 1.4% Mn and for TWIP steels having 0.6% C, adapted from Barrie Mintz [5] (2022) in which precipitation hardening is not contributing to the RA value, adapted with permission from [2], 2010, Taylor & Francis.

However, weakening the grain boundaries by having residual amounts of Cu, As, Pb, P, and S segregated there can also contribute to a deepening of the trough, leading to intergranular failure [7,8]. Hence, it is not essential to have the thin film of ferrite present to give poor ductility, and other explanations are given; these being precipitate-free soft zones (PFZ) near the boundaries, low melting point phases precipitated at the boundaries, or weakening of the metallic bonding at the boundaries by the segregation of foreign atoms. In the case of B additions to steel, the latter explanation is often given, this time for strengthening the bonding [2,8].

It is generally found in steel that the changeover from transgranular ductile to intergranular brittle occurs when the RA value using a standardised tensile testing regime drops below 35% and almost fully brittle failures occur when the RA value is <20% [9].

However, these other explanations for intergranular failure are very different to the concept of soft films of ferrite being responsible for the trough. Intergranular failure when the thin film is present is ductile and is caused, on deformation, by voids forming around the MnS particles at the boundaries, linking up in a ductile manner to give fracture [6]. The reason ductility is so low is that most of the total strain is taken up by the ferrite film. The failure here is low-ductility “ductile” intergranular, not brittle intergranular. However, even when “ductile” intergranular failure occurs, Ouchi and Matsumoto [10] clearly showed that GBS, as seen in Figure 3, still contributes very much to the failure at these elevated temperatures (700–1000 °C) and accounts for its intergranular appearance. Therefore, even when the film of ferrite is present and the fracture is ductile-intergranular, GBS is still operative. They make the point that austenitic grain boundary sliding may be a necessary condition for initiating a crack, but it is not always the controlling factor for propagation and hot ductility [10].

Troughs in which no ferrite films are present are shown in Figures 4 and 5 for fully austenitic and fully ferritic steels, respectively [11]. The troughs in these two steels are due to dynamic precipitation of fine carbides and nitrides forming at the grain boundaries. Ductility improves at the high-temperature side of the trough where the precipitates are too coarse to influence ductility and at the low-temperature side, when they are not precipitated out in the time of the test.

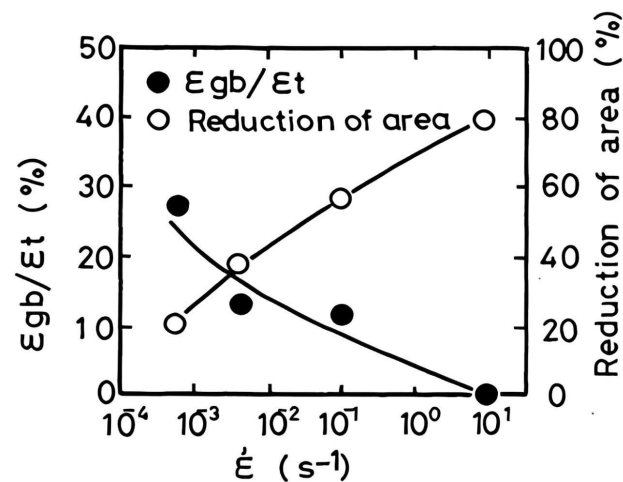


Figure 3. The effect of strain rate ($\dot{\epsilon}$) on the hot ductility and grain boundary sliding in a Nb containing (0.054% Nb) HSLA steel tested at 800 °C (ϵ_t is the strain in the tensile test and ϵ_{gb} is the strain due to grain boundary sliding), adapted with permission from [10], 1982, Transactions of the iron and steel institute of Japan.

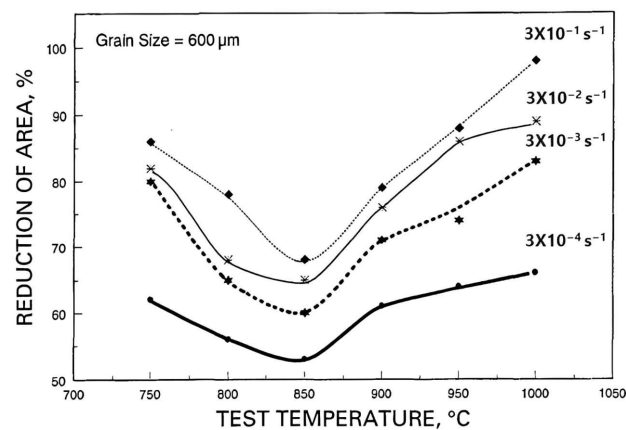


Figure 4. Hot-ductility curves for coarse-grained (600 μm) austenitic stainless steel for four strain rates. The composition of the steel was 0.014% C, 25.5% Cr, 22% Ni, 2% Mo, 0.11% V, and 0.13% N, adapted with permission from [11], 1997, Taylor & Francis.

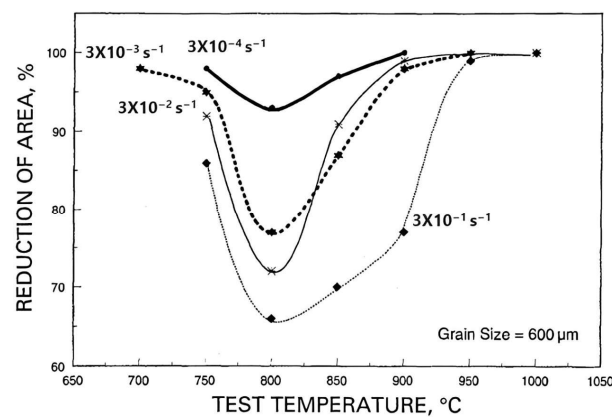


Figure 5. Hot-ductility curves for coarse-grained (600 μm) ferritic stainless steel at the same four strain rates used for the austenitic stainless steel. The composition of the steel was 0.013% C, 18.5% Cr, 2.3% Mo, 0.02% Nb, 0.28% Ti, and 0.013% N, adapted with permission from [11], 1997, Taylor & Francis.

However, the effect of strain rate on the hot ductility of coarse-grained fully austenitic (fcc) and fully ferritic (bcc) steels is very different, as shown above in Figures 4 and 5. In the case of the austenitic steel, increasing the strain rate improves ductility, while for the ferritic steel, ductility deteriorates. This illustrates the difference between when fracture is controlled by GBS, as it is with austenite, and when it is not, as in ferrite. For austenite, GBS occurs easily so that increasing the strain rate reduces the amount of GBS and ductility improves (see Figure 4). In contrast, with a ferritic stainless steel, increasing the strain rate causes the hot ductility to decrease and failure is transgranular, as is normally found when testing at room temperature (see Figure 5). This arises because when tensile testing at elevated temperatures, both GBS and DRX have difficulty occurring in a ferritic structure [12,13] and the ductility is controlled by the inclusions and the dislocation density, in the same way as it is at room temperature. In an austenitic structure, DRX is favoured as the softening process, whereas DRV is favoured in a ferritic structure [12,13]. For ferritic structures, increasing the strain rate causes the dislocation density to increase, encouraging fracture (unless recovery is very rapid).

In the case of the ferritic stainless, Figure 5, which contains Nb as a microalloying addition, the poor ductility is caused by the dynamic precipitation of Nb(CN), and for the austenitic steel, Figure 4, which contains V as a microalloying addition, it is probably the precipitation of V(CN) [11]. The failure mode is mainly transgranular in the ferritic steel as the minimum ductility is always high, $\geq 65\%$. It is the precipitation and inclusions within the matrix rather than at the boundaries that are influencing ductility. In the matrix, when precipitation is at its finest, the dislocation density will be high, embrittling the steel, but at higher temperatures the particles are too coarse to influence ductility. At lower temperatures there are no or too few precipitates to influence ductility. In contrast, for the austenitic stainless steel, GBS dominates the fracture process.

However, Liu et al. [14] gave a totally different explanation to account for the hot-ductility troughs and the influence of strain rate in these fully austenitic and ferritic steels. This theory is not based on precipitation but assumes the trough is caused by P segregation to the boundaries weakening the bonding there. The trough can then be explained by the non-equilibrium segregation of P to the boundaries, with the RA value decreasing as the amount of P segregated to the boundaries increases. For non-equilibrium segregation, there is a critical time for reaching the maximum segregation, corresponding to the worst ductility. At greater times, back-diffusion of P from the boundary takes place and the P level at the boundaries decreases and ductility improves. This critical time can be accurately calculated from the processing times used for the tensile test, and this can then be used to explain the shape of the hot-ductility troughs and the influence of strain rate as well as the influence of strain rate on grain size. The time required for back-diffusion of P to occur from the boundaries leading to less P and better ductility is very different for the two steels, being much faster in a bcc structure compared to an fcc structure [15]. Xu et al. [16] came to similar conclusions with regards to the importance of non-equilibrium segregation in accounting for intergranular embrittlement.

Hence, intermediate-temperature embrittlement in steels can also be caused by the segregation of trace elements to the boundary either weakening or strengthening the boundary. B is an example for strengthening [2,15] and S [17–19] and Sn for weakening [15]. Kang et al. [17] showed, using auger electron spectroscopy (AES), that the ductility loss that they found in plain low-C-Mn steels (0.04% C, 0.46% Mn) on cooling from 1400 °C to 1000 °C can be ascribed to the segregation of free S to the austenite grain boundaries, and this high-temperature embrittlement by S to the grain boundaries is often reported. [2,18,19]. Laha et al. [18], using AES, detected both S and O₂ on an austenitic Ni-Cr-Fe weld fracture surface showing poor ductility, and Heo et al. [19] found that ductility improved in a type 347 austenitic stainless steel when B and Ce were added. The Ce was needed to remove the S to allow the B to segregate unimpeded to the boundaries.

Another type of high-temperature intergranular failure in steels is the segregation of elements which form low melting point compounds at the grain boundaries and, hence,

give rise to a hot-ductility trough. In steels, P [20] and Cu [21] are the main elements causing such a problem. A residual level as low as 0.01% Cu can lead to hot shortness in steel, allowing the low-melting-point Cu phase to form, which melts on hot rolling, leading to cracking. Similarly, P, when segregated in excess to the boundaries, forms a low-melting-point iron phosphate compound. Hot ductility, like hot shortness at the low strain rates, typically used in the straightening operation, is also affected by these elements, and although its origins may be similar, there is no conclusive evidence [20]. Furthermore, P segregation can, at times, benefit hot ductility [22].

3. Troughs in Spheroidal Cast Irons

Mg is added to iron to spheroidise the graphite ($\geq 0.04\%$ Mg), thus improving the room-temperature ductility and impact resistance. However, a Mg addition can cause embrittlement at elevated temperatures [23]. Like steel, spheroidal graphite cast iron is susceptible to this intermediate-temperature embrittlement, but at a lower temperature range of 350–500 °C, compared to 700–900 °C, for low-C steel (i.e., melting point of cast iron and low C steel, ~1050 and 1540 °C, respectively) [24–30]. Wright and Farrell [24] showed that this embrittlement increases with Mg and S content, but adjusting the P level can restore the ductility.

Similarly, Iwabuchi and Kobayshi [27] showed that increasing the Mg content at the same P level, Figure 6, curves C and F, caused the trough to deepen and widen, whilst increasing the P level at the same Mg level caused the ductility to improve (curves A and C). They examined a number of cast irons with various combinations of P (0.07–0.14%) and Mg (0.037–0.085%), and concluded from their work that the elevated temperature brittleness shown in Figure 6 and the intergranular fractures associated with the trough were probably due to segregation of Mg (i.e., Mg has a melting point of 650 °C) to the boundaries, weakening the bonding there and occurring when the Mg%/P% ratio is >1.5 . P is beneficial because it probably segregates preferentially to the boundaries before Mg is able to reach them, removing the vacant sites needed for segregation of Mg to occur and so strengthens the boundaries. This beneficial effect of P segregation is a consequence of its high diffusion rate [31]. A similar benefit is found when the P level is increased in HSLA steels, preventing the more deleterious to ductility Nb precipitating out as carbides on the vacant sites [7]. However, if too much segregation of P to the grain boundary occurs, the low-melting-point iron phosphate type phase forms, giving liquid films, very low ductility, and intergranular failure [20].

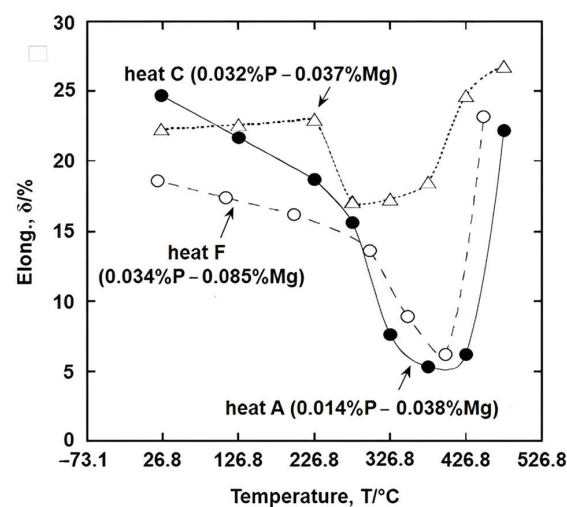


Figure 6. Hot-ductility curves for spheroidal cast iron showing the beneficial effect of P in righting the detrimental effect of Mg, adapted with permission from [25], 2023, Elsevier. The strain rate used was $3 \times 10^{-4} \text{ s}^{-1}$. The base composition was 3.5% C, 2.6% Si, 0.05% Mn, 0.005% S, and 0.028% Ni.

Chen et al. [28] further confirmed, using AES, that P does segregate to the ferrite grain boundaries in cast irons. However, Gonzalez-Martinez et al. [25] more recently suggested that the embrittlement is due to oxygen infiltration from the atmosphere to the grain boundaries, which then combines with the Mg there, forming brittle MgO particles. It is not clear why the particles have to be brittle to influence crack growth. These coarsen with increasing temperature, thus improving ductility. The reason for Mg causing such a detrimental effect on ductility is still, therefore, unclear, but Seah [32] calculated, from his theory that relates segregation to the strength of grain boundaries, that Mg is likely to be one of the most detrimental of elements when segregated to the boundaries for weakening their bonding.

Because the lower testing temperatures used for cast iron are within the temperature range for dynamic strain ageing (DSA), fracture examination showed cleavage fractures even at as low a strain rate as $3 \times 10^{-4} \text{ s}^{-1}$ (Figure 7a) [25]. The fracture appearance can be seen to gradually change from cleavage to intergranular with increase in temperature; Figure 7b. At the highest test temperature, the fracture appearance was ductile transgranular; Figure 7c [25]. The cleavage fractures gave slightly better ductility than intergranular failures but only because the RA values were very low, ~10% RA, as seen in Figure 7a and b. It is not too surprising that cleavage fractures have at times better ductility than intergranular failures. Cleavage fracture is transgranular and takes place along the (100) planes in bcc metals. Crack propagation depends on the bonding between the planes, the rapid build-up of dislocations, and the sharpness of the crack front. Intergranular fracture depends on the bonding at the boundaries, and if, for example, in an extreme case, there is a wafer-thin film of liquid covering the solid grain surfaces, the energy required for crack propagation will be very low, and less than that for cleavage.

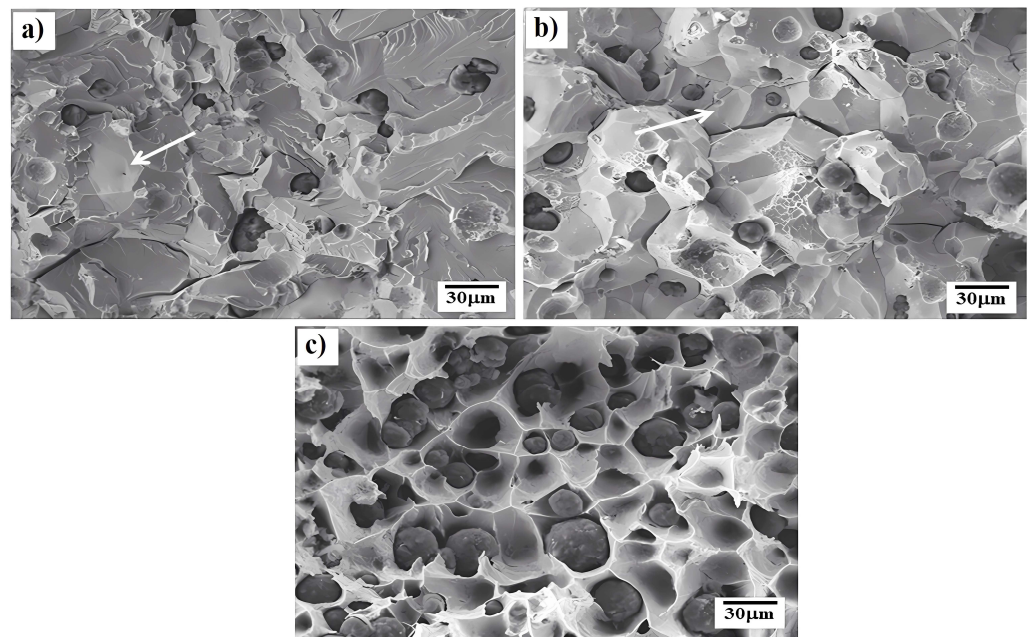


Figure 7. The different kinds of fracture that were found on the fracture surface in spheroidal cast iron: (a) cleavage fracture at RT, (b) intergranular fracture at 475 °C, and (c) ductile fracture at 650 °C. The black spheres are spheroidised iron carbides. Specimens were machined after casting and tested at temperatures in the range RT to 650 °C at a strain rate of $3 \times 10^{-4} \text{ s}^{-1}$. Composition of the cast iron was 3% C, 5% Si, and 0.038% Mg, adapted with permission from [25], 2023, Elsevier.

In the case of spheroidal cast iron, the matrix ferrite structure is bcc and intergranular failure is caused by the segregation to the boundaries of undesirable elements that influence the cohesion of the grains, rather than GBS, although GBS probably still plays a part. For these alloys, it is clear that Mg [24–26,29] is particularly detrimental to the ductility, whilst

P has been shown to be beneficial [24,27,28]. S has also been shown to be detrimental to hot ductility [24]. Yanagisawa et al. [29] detected both Mg and P at the boundaries, which may indicate the formation of Mg_3P_2 , suggesting that P may remove Mg atoms from the boundaries, thus improving ductility. Finally, as with refining the as-cast austenite grain size in steels, refining the dendritic ferrite grain size improves ductility [29].

Although, it is shown in Figure 6 that Mg deteriorates the ductility, whereas P improves it, as with so much of this work, the reason for their influence is often unclear. The explanations range from one of oxygen infiltrating from the atmosphere combining with the Mg segregated at the boundaries to the Mg at the boundaries combining with the P. The authors of this paper suggest another possibility, which is that P may benefit the ductility because its rapid diffusion rate [30] enables it to reach the oxygen at the boundaries before the more detrimental to ductility Mg reaches it, and P, being a metalloid, can combine with oxygen, forming a pentoxide.

4. Troughs in Aluminium Alloys

Ductility troughs are again present in some Al alloys, particularly in Al-Mg alloys, and the RA values, on occasions, can be almost zero [33–35].

Al-Mg alloys have high strength, excellent corrosion and fatigue resistance, and good welding performance and are extensively used in structural applications in the marine, automotive, and aeronautical industries, where weight reduction is an important factor [36–40]. However, coarse-grained Al-Mg alloys, particularly with more than 5% Mg, are susceptible to high-temperature embrittlement, and considerable research has been carried out into finding out the cause, as it can result in edge cracking on hot rolling [40,41].

Much of the early work [28,33,34,42] to assess the hot ductility of these alloys was carried out using tensile specimens that were strained at a low strain rate of $\sim 10^{-4} \text{ s}^{-1}$. It was established from this work that the main element deteriorating the ductility was Na, which, even in the trace amounts introduced during the Al-Mg alloy processing route, deteriorated the hot ductility. For example, in an Al-Mg-Si alloy, as little as 20 ppm Na was enough to cause embrittlement at the boundaries, forming a liquid, giving intergranular failure. It was suggested that Na atoms segregated to the boundaries, forming molecules which melted during hot rolling (i.e., the melting point of Na is 97.8°C) [35,42]. However, hydrogen cracking caused by hydrogen absorption from water vapour in the atmosphere has also been cited as part of the cause when melting is carried out in air [43,44].

Because of the detrimental effect Na has on ductility, much of the scientific work has been devoted to finding elements which counteract this deterioration. Horikawa et al. [34,35,45] examined the hot ductility of a variety of trace elements, Ca, Sr, Li, Si, and Na, in an Al-5% Mg alloy [34,45]. The curves for the Sr and Ca additions are shown in Figure 8a,b, respectively, and they show that when Na is not present, these elements themselves are detrimental to ductility but not as detrimental as when as little as 2 ppm of Na is present in the alloy [35]. A similar detrimental behaviour to ductility, as shown by Sr, was noted for Li (curve not shown) [35]. From all of the elements they examined, Si was the only one benefitting ductility and preventing the embrittlement by Na; Figure 8c [35]. On the beneficial side, Okada and Kanno [33] found that an addition of 0.04% Y completely removed the trough for an Al-5% Mg alloy containing 0.06 ppm of Na, but no improvement was noted at a higher Na level of 0.60 ppm. Y is very efficient in removing hydrogen in the melt [46], thus preventing hydrogen cracking from occurring, but this was not the cause of the improvement in ductility in this Al-5% Mg, Na-containing alloy, as embrittlement still occurred even when hydrogen was not allowed to enter the melt from the atmosphere. It was suggested that both hydrogen and sodium needed to be removed to prevent embrittlement, and Y somehow removed the detrimental influence of Na [33]. A small addition of Bi or Sb (ppm) has also been found to be beneficial [47]. In the case of Bi, it was shown that Bi could combine with Na to form a NaBi compound and hence remove the Na from solution [47]. Similarly, Sb probably acts in the same way [48]. The explanation given for Si improving the ductility was that the impurity elements were all able to segregate to

the periphery of the Mg_2Si particles in the matrix, instead of going to the boundaries and weakening them [34].

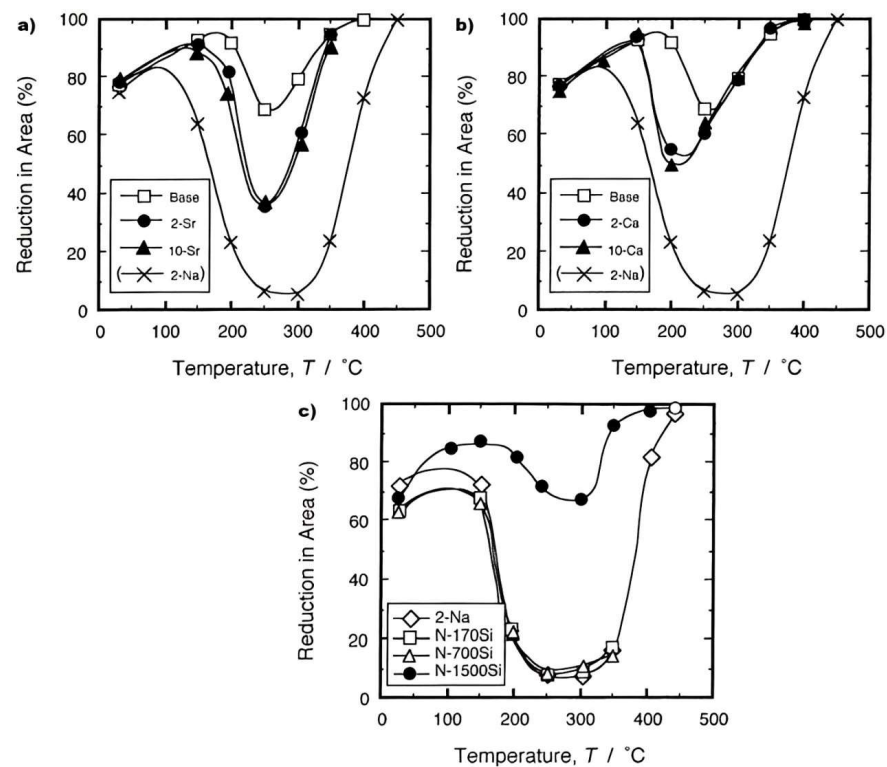


Figure 8. Influence of (a) strontium, (b) calcium, and (c) silicon on the hot ductility of Al-5% Mg. The influence of Na at 2 ppm (mass) is shown for comparison. Numbers adjacent to the elements are in ppm, adapted with permission from [45], 2001, Elsevier.

All these research papers suggest that ductility is very much influenced by segregation of elements to the grain boundaries, which can weaken or strengthen them. Lynch [49] made the important point that embrittlement involves the transport of impurity atoms to the crack tips where they are absorbed, so that they weaken the bonding at the boundary, enabling the cracks to grow quickly by decohesion or dislocation emission. Suzuki et al. [50] suggested that the weakening or strengthening at the boundary depends on the valence electron density there; strengthening when the impurity atoms had more valence electrons than the matrix and weakening when they contributed less. The model here is based on the matrix positive metal ions being held together by a sea of negative electrons. At the boundaries, bonding can only take place with the valence electrons so the more of these there are, the stronger is the boundary.

In the case of contamination by Na, the fracture surfaces after testing at 300 °C, the temperature showing the worst ductility, were either very flat intercrystalline at the higher Na level, Figure 9a, or microvoid coalescent ductile at very low Na contents, Figure 9b [45]. Although the poor ductility is often ascribed to the segregation of sodium to the grain boundaries (Na having a very low melting point of 98 °C), AES has never detected Na on the grain surfaces [35,45], and this explanation does not account for recovery in ductility at the higher temperatures. This led Zhang et al. [40] to look at the thermodynamics more closely, and they showed that in the Al-5Mg-Na ternary diagram, there is a window in which there is a liquid temperature range (see Figure 10a) before the fcc solid structure transforms at the lower temperature to the bcc solid structure. This liquid range then becomes more extensive and deeper as the Na level increases (see Figure 10b). The Na level needs to be <0.5 ppm before the RA value is >35%, and failure is transgranular ductile. This theory would, which many others do not, account for ductility improving at both the high-

and low-temperature ends of the trough when solid fcc and solid bcc phases are present, respectively. However, Lynch [49] suggested that the hot-ductility trough in these Al-Mg alloys could also be explained on the basis of GBS and recovery, in that there is a critical balance between the two processes. At low temperatures, GBS cannot occur, so ductility is high. At intermediate temperatures, GBS occurs and dominates ductility, so ductility is poor. At high temperatures, recovery processes occur too quickly for GBS to let cracks grow, and there is often migration of the boundaries away from a growing crack such that ductility is very good. Lynch [49] also noted that in the brittle region, the grain boundaries are serrated, indicating that there will be high local stresses encouraging cavitation and GBS. However, the very flat, shiny, glassy surfaces on the fracture surfaces (Figure 9a) do tend to suggest that there may have been a very thin film of liquid trapped between the grains, making GBS very easy.

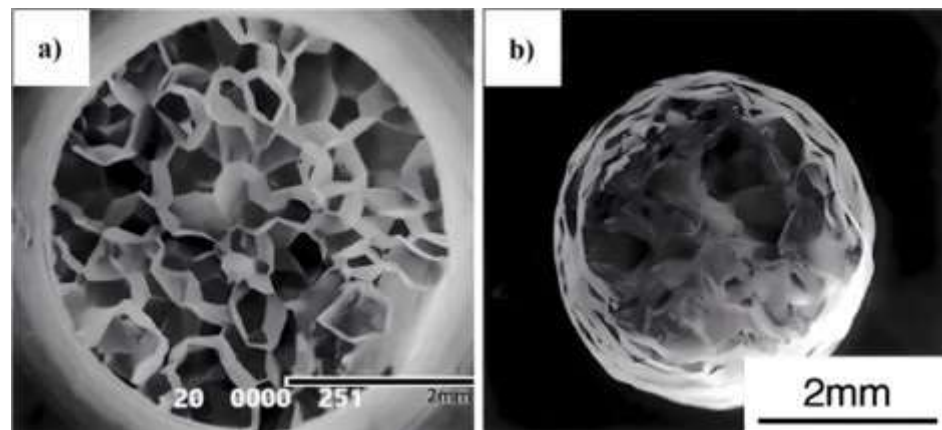


Figure 9. Fracture surfaces of an Al-5.5 mol% Mg alloy tested at 300 °C at a strain rate of $\sim 10^{-3} \text{ s}^{-1}$ with (a) 1.8 mass ppm Na, intergranular fracture, and (b) 0.1 mass ppm Na, mainly transgranular ductile failure, adapted with permission from [45], 2001, Elsevier.

There is always the added influence when melting is carried out in contact with the atmosphere that the weakening of the boundaries may also be enhanced by oxygen or hydrogen absorption from the atmosphere, as at these elevated temperatures these atoms can very easily diffuse and, on reaching the boundary, can form molecules, and the expansion there can open up the cracks [33,43,44].

For these Al alloys, Hammad and Ramadan [51] found that increasing the strain rate in the range 5.5×10^{-5} to $5.5 \times 10^{-3} \text{ s}^{-1}$ decreased the hot ductility, as measured by elongation in an Al-3% Mg alloy. The alloy was solution treated and water quenched and tensile tested in the temperature range 27 to 530 °C. The high-temperature embrittlement was suggested as being due to precipitation of Al_3Mg_2 and Mg_5Al_3 compounds.

Deschamps et al. [41] also showed that in an Al-Mg-Mn alloy the strain rate has a marked influence on the fracture appearance and ductility. At low strain rate (0.02 s^{-1}) in the temperature range 500–550 °C, ductility was high, 60% RA, and fractures were transgranular ductile. As the strain rate increased from 0.02 to 5 s^{-1} for a test temperature of 500 °C, the fracture gradually changed from transgranular ductile to brittle intergranular, with the ductility falling from 60 to 20% RA. Surprisingly, at the very high strain rates of 10^{10} to 10^{25} s^{-1} , testing at 500 °C, the fracture again changed in appearance to a mixture of brittle intergranular and brittle cleavage, giving the lowest RA of 10%. The cleavage fractures were probably caused by the localised melting at the grain boundaries forming a very sharp crack with a high stress concentration [41].

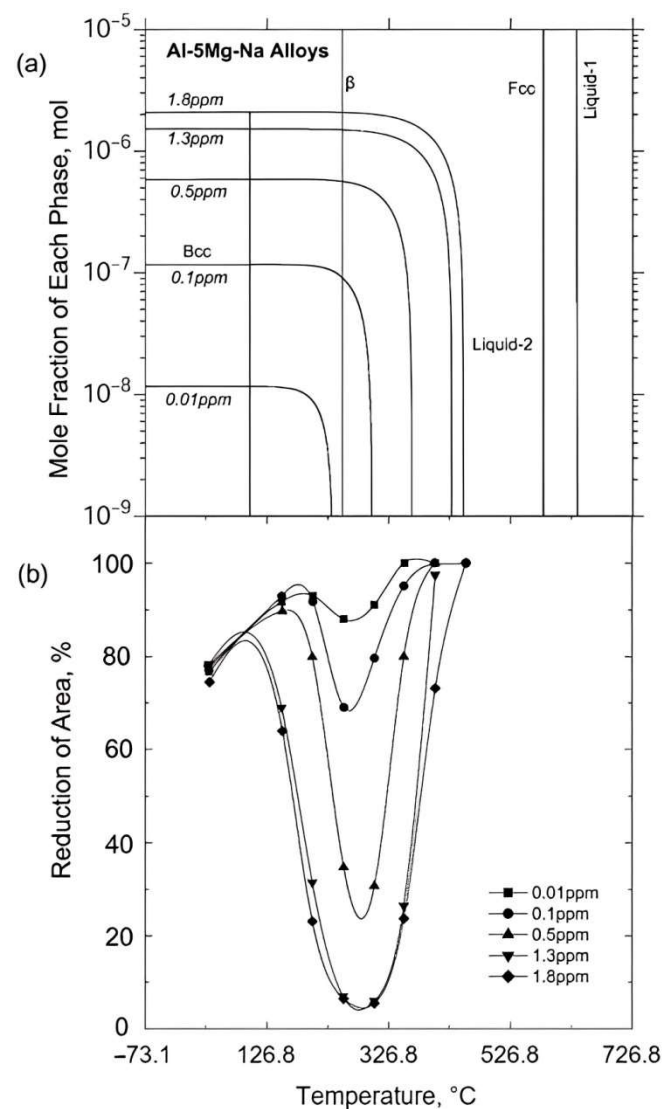


Figure 10. Calculated phase relations in comparison with experimental data on RA. (a) Calculated mole fraction of each phase versus temperature curves during solidification of Al-5Mg-Na alloys with different Na contents, reprint with permission from [41], 2002, Taylor & Francis. (b) Effect of Na content on hot ductility of Al-5Mg alloys at different temperatures, adapted with permission from [35], 1998, Keikinzoku.

It is perhaps useful at this point to note that Al-Cu alloys also have a hot-ductility trough in the temperature range 100 to 500 °C, with the minimum ductility being at ~250 °C. Lin et al. [52] investigated the tensile behaviour in the lower-temperature range 100–250 °C, and Liu et al. [53] examined the higher-temperature range 250 to 500 °C. In the lower-temperature range (100–250 °C), Lin et al. [52] found the elongation to increase with the decrease in temperature or increase in strain rate in the range 3×10^{-3} to $3 \times 10^{-5} \text{ s}^{-1}$. This is because, for the elongation, the work hardening rate increases with lowering of the temperature, and eventually outweighs the lack of any recovery. Increasing the strain rate gives less time for recovery processes to take place in the timeframe of the deformation process. Although some recrystallisation was observed at the highest temperature, 250 °C, recovery was the main mode of removing dislocations. Furthermore, Liu et al. [54] found, at the higher temperature range of the trough 250 to 500 °C, that, again, the main softening mechanism was DRV. The effect of increasing the strain rate on hot ductility of the Al-Mg alloys is therefore the opposite to that of the Al-Cu alloy. This influence of increasing strain rate in decreasing the ductility in Al-Mg alloy is more in keeping with the behaviour shown

by ferritic steels, whereas for the Al-Cu alloy, it is more in keeping with the behaviour shown by austenitic steels in which GBS is the major cause of failure.

Finally, for this section, as with steel, coarsening the grain size embrittles the alloy [55].

5. Troughs in Copper Alloys

Again, hot-ductility troughs are present, and segregation to the grain boundaries influences the depth, giving typical intergranular and transgranular fractures, as found in steel. Data on hot ductility are sparse because although there are generally no cracking problems, the occasional presence of undesirable impurity segregates to the grain boundaries can give rise to a hot-ductility trough, as shown in Figure 11 for residual lead.

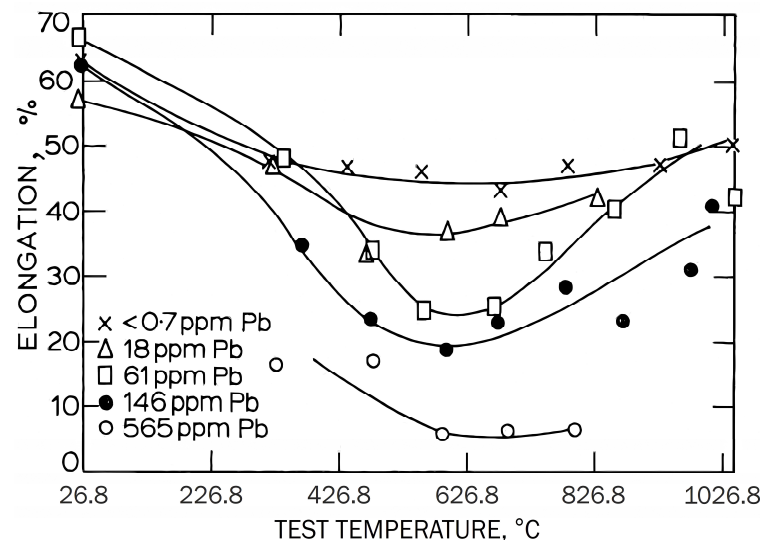


Figure 11. Effect of lead additions on ductility–temperature behaviour of a Cu-10Ni alloy. A high strain rate of 10 s^{-1} was used, reprint with permission from [56], 1984, Japan Institute of Metals.

Gavin et al. [56] also showed that in an as-cast Cu-10Ni alloy the depth of the intermediate-temperature trough, using the elongation as a measure of ductility, was adversely affected by the impurity elements studied (i.e., Bi, Pb, Se, S, and Te). It is important to mention that a high strain rate of 10 s^{-1} was used. The impurity levels varied from 1 to 750 ppm (wt.%). S was relatively innocuous at levels as high as 750 ppm (wt.%). The fracture appearance was ductile transgranular at the low- and high-temperature ends of the trough, and at the intermediate temperatures, the fracture became more and more intergranular with impurity content and decrease in ductility. They suggested that the impurity elements segregate to the grain boundaries and weaken the bonding, but no direct proof was offered.

The improvement in ductility occurred for this Cu-Ni alloy, as for steel, when recrystallization was possible. Chubb and Billingham [57], using a similar testing procedure to the previous reference, found that in Cu-Ni alloys the ductility decreases with Ni content, and suggested that this is because Ni delays the recovery and recrystallisation processes. As with steel, there is a minimum ductility, in this case, 30% elongation, when the fracture appearance changes from transgranular to intergranular.

6. Ni and Nickel Alloys

Ni and Ni alloys are used in the aerospace industry for turbine blades, discs, and parts close to the aircraft engine, having high strength, fatigue and corrosion resistance, and, most importantly, good creep properties at high temperatures. However, Ni-based superalloys are prone to high-temperature embrittlement in the intermediate-temperature range 600 to 900 °C unless precautions are taken [58,59]. Ni-based superalloys are used at temperatures of 650–700 °C and sometimes reach as high as 800 °C [60].

Hu et al. [60] showed that Ni-Co-based superalloys have very poor ductility, <5% elongation, at temperatures in this temperature range, as shown in Figure 12. The fracture surface gradually changed from ductile to intergranular brittle as the tensile testing temperature increased from room to 750 °C when decohesion took place at the interface between the γ' precipitates and the γ matrix on the fracture surface. In this case, the poor ductility was ascribed to the prolific precipitation of γ' in it various forms and the low stacking fault energy, which produced a vast number of deformation twins when a change in the mode of deformation took place at high temperatures [60].

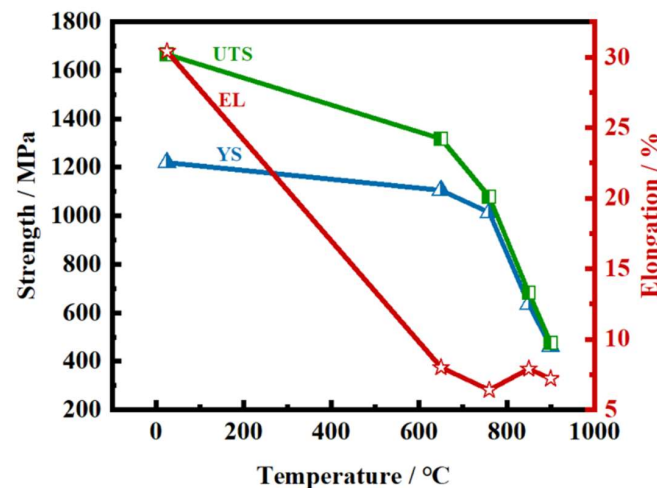


Figure 12. Tensile properties of a Ni-Co-based superalloy using a strain rate of $3 \times 10^{-4} \text{ s}^{-1}$ (composition: 25% Ni, 14% Cr, 2.8% Mo, 1.2% W, 8.0% (Al, Ti, Nb), 0.02% C, 0.02% B, 0.03% Zr, and balance Ni, adapted from [60], 2022, Crystals.

White et al. [61] examined the high-temperature embrittlement of Ni and Ni-Cr alloys. Trace elements were found to influence the creep cavitation process and AES was used to provide direct evidence of impurity segregation to the cavity surfaces at the boundaries. Trace additions of Sb and Sn (1 wt.%) caused extensive creep cavitation whilst 0.11% Zr, in contrast, inhibited creep. Residual S when it was over 10 ppm was the main segregate causing problems, as shown in Figure 13 [61,62]. The importance of GBS and the effect of impurity elements on weakening or strengthening the boundaries were again highlighted.

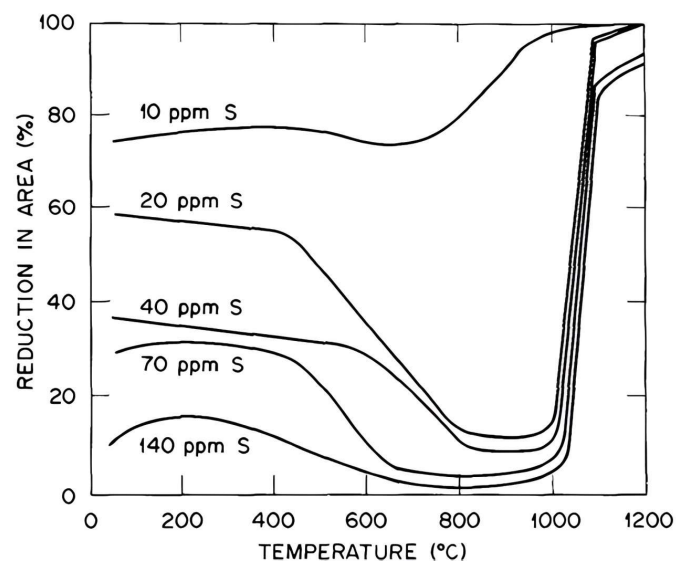


Figure 13. Reduction in area plotted vs. temperature for nickel, at various concentration of sulphur, adapted with permission from [61,62], 1983, Springer.

This very detrimental effect of S seems to be very common in alloys, and Christien [63] reported, (Figure 14) a similar effect in an austenitic Fe-Ni alloy (42% Ni). This gave a similar hot-ductility trough to those shown above in Figure 13, but almost zero ductility occurred at a test temperature of 800 °C, with S levels as low as 9 ppm when tested at a strain rate of $8 \times 10^{-5} \text{ s}^{-1}$. Increasing the strain rate had a marked influence in restoring ductility, as it does for austenitic steel. Christien [63] also suggested that the transport of S to the crack tip under deformation is extremely fast, leading to a significant reduction in the surface energy, facilitating crack growth. Increasing the strain rate results in the S level at the crack tip being decreased, leading to better ductility.

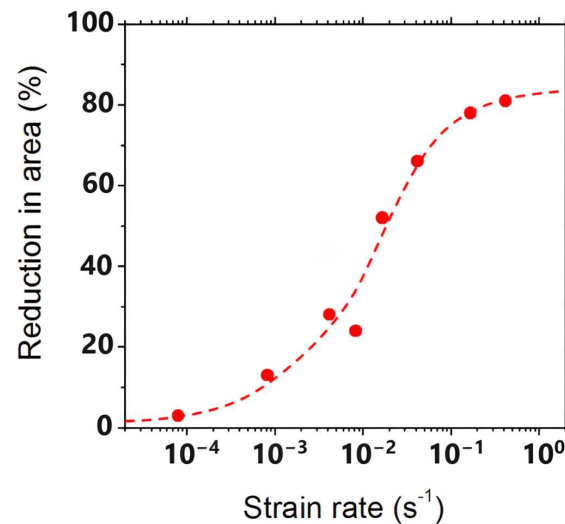


Figure 14. Influence of strain rate on the RA of a Fe-Ni alloy with 9 ppm of S tested at 850 °C. A preheating step at 850 °C was conducted so that the total time spent at 850 °C was the same for all tests of 40 min, adapted from [63], 2020, Materials.

Oxygen can also cause cracking if precautions are not taken, as Figure 15 shows [64], and hydrogen cracking after aging has been found in Ni-based alloys [65]. However, Bricknell and Woodford [64] found little influence of strain rate in the range 10^{-2} to 10^{-4} s^{-1} on the elongation.

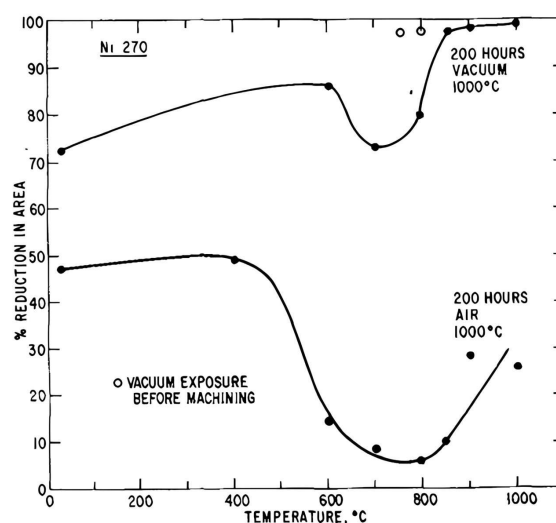


Figure 15. Hot-ductility curves of %RA against temperature for Ni270 tested in temperature range of RT to 1000 °C following 200 h air or vacuum exposure at 1000 °C. Also shown is the beneficial effect of machining samples from the centre of blanks after vacuum exposure. A strain rate of 10^{-3} s^{-1} was used, adapted with permission from [64], 1981, Springer.

7. Discussion

Origin of the Troughs and Intermediate-Temperature Embrittlement

It is clear from the foregoing that hot ductility of alloys is very complex and there is no one unifying interpretation. There are many causes of the trough and intermediate-temperature embrittlement; the soft film of ferrite (as in the case of steels), precipitation, presence of precipitate free zones (PFZs), melting of the solute at the boundaries, the change from dynamic recrystallisation (DRX) to dynamic recovery (DRV), and GBS, and, very often, segregation to the grain boundaries is needed to give a trough. Thus, it is not surprising that there is a multitude of explanations for a hot-ductility trough.

However, there are two common conditions required for a trough to appear and the ductility at the base to be poor, resulting in intergranular failure. The first is that embrittlement, which gives intergranular failure, usually involves GBS in fcc alloys including austenitic steels. This means that it normally only occurs when conditions are ripe for creep, i.e., the homologous temperature is 0.3 to 0.5 T_m . The second, and most important, requirement is that there must be some weakness at the boundaries and this can take many forms, from segregation of impurity atoms to the boundaries, to soft films of ferrite, to liquid films at the boundaries.

It must be stressed that the conditions are critical and, for example, GBS, as well as causing embrittlement, can also give rise to superplasticity [66]. As long as the GBS is controlled so it does not develop cracks, which lead to fracture, enhanced ductility can occur [66]. Al-4.5% Mg can give 300% elongation when tested at a strain rate of 10^{-3} s^{-1} at 400 °C. In this alloy, the strain rate sensitivity is high and necking is prevented [66]. Similarly, as well as impurity elements, which segregate to the boundaries, weakening them, there are others which will strengthen the boundaries. Design of engineering alloys (DEA) [67–74] has now become an important field of research with tremendous potential not only for improving the elevated temperature properties of metals and alloys but also improving the room temperature properties. He et al. [72] noted that although a lot is known about grain boundary strengthening, little attention has been paid to its effect on mechanical properties, and this is an obvious area for more research. DEA has been used to develop high-entropy alloys (HEA) composed of multiple principal elements with exceptionally high strength and thermal stability, and the optimum strength for these alloys has been derived theoretically and confirmed experimentally, but these are isolated cases [73,74]. DEA also has been used to optimise room-temperature strength in high-entropy nano-polycrystalline alloys having Fe, Al, Ni, Cr, and Cu present [72,74]. Cu was shown to be the main element that segregates to the boundaries and strengthens them, but the amount segregating has to be closely controlled, as too much weakens the boundary. Lejcek et al. [70,71] made considerable headway in relating interfacial segregation to grain boundary embrittlement in bcc iron, and there is considerable agreement with the experimental observations and theoretical calculations.

In low- to medium-C steel, the hot ductility after casting is often controlled by the formation of the soft, thin film of DIF, and this has tended to dominate research on the subject, but this, as already noted, is not essential for a hot-ductility trough to be present, even in steels. PFZs are often present in many alloys, and then the hot-ductility behaviour becomes very similar to having the soft ferrite film at the boundaries. Fracture is then similarly low ductility, but “ductile” intergranular. These PFZs not only occur in austenite but are present in most alloys when dynamic precipitation can take place.

In discussing these hot-ductility curves, it is important to address the different factors that influence their formation and control the shape and depth, these being composition, grain size, strain rate, and precipitation.

8. Influence of Composition, Grain Size, Strain Rate, and Precipitation on Hot Ductility

For low- to medium-C steel, the width of the trough is related to when the ferrite film forms and so is related to the austenite to ferrite transformation, which has been shown to be defined generally as the temperature range from the A_{r3} to the A_{e3} when DIF can

form [2]. DIF is believed to form very easily, and only a small deformation is required (2–3%); hence, it is present during the straightening operation when continuously casting steel [2,75]. The composition of the steel is therefore important, particularly the C and Mn contents, the elements which have the major influence on the transformation temperatures. When no C is present, i.e., pure iron, no films can form, and ductility is 100%, even at low strain rates, 10^{-3} s^{-1} .

More generally for alloys with microalloying elements, the width is the range of temperature in which fine dynamically precipitated precipitation can occur. When liquid films form at the boundaries, it is at the range of temperature in which the molten liquid is stable.

8.1. Grain Size

In this rather confusing research field of hot ductility, of all the many variables influencing this, refining the grain size seems to invariably improve the hot ductility, although its effect can vary considerably, with the improvement increasing as the grain size decreases, as the curve in Figure 2 shows [2]. Thus, for steels, refining the grain size from 1000 to 300 μm only has a relatively small influence in improving ductility, but refining the grain size from 300 to 80 μm has a major influence. Hence, refining the as-cast grain size from 600 μm , as in Figures 4 and 5, to $\sim 30 \mu\text{m}$, which is shown in Figure 16a,b, completely removed the troughs in both the fully ferritic and fully austenitic steels, independent of the strain rate in the range examined [11].

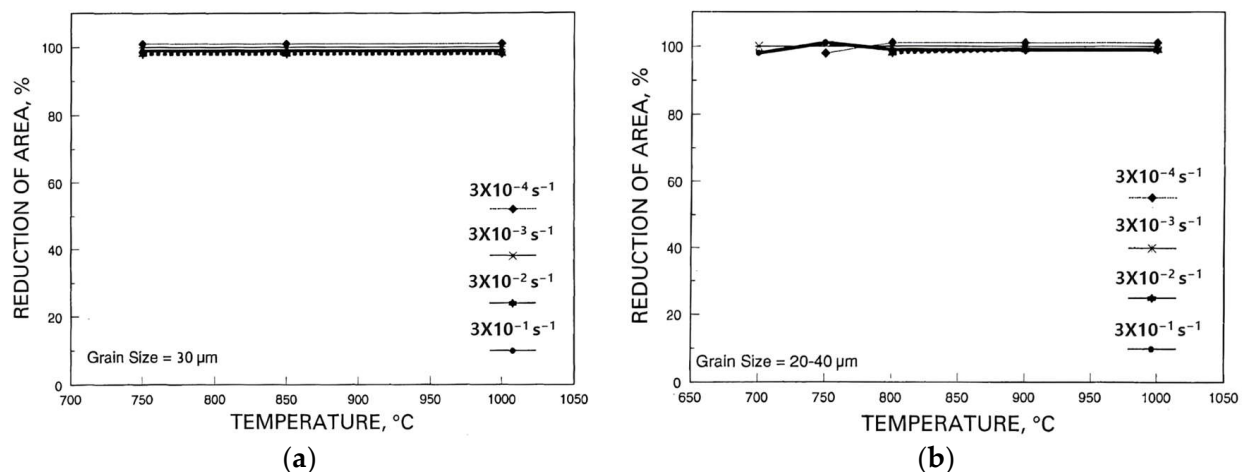


Figure 16. Powerful influence of refining the grain size from 600 μm to $\sim 30 \mu\text{m}$ in removing the trough both in (a) fully austenitic (fcc) and (b) fully ferritic (bcc) steel, adapted with permission from [11], 1997, Taylor & Francis.

8.2. Strain Rate

The influence of strain rate is variable in these alloys, sometimes having little or no influence [66], improving ductility or making it worse [11].

When creep conditions apply as with austenite, increasing the strain rate will improve hot ductility but in their absence normal transgranular ductile failure is likely to occur.

However, when liquid films are present or the bonding is severely weakened at the boundaries by trace impurities, increasing the strain rate is likely to be beneficial because less time is available for the weakening segregates to reach the boundaries.

In coarse-grained low- to medium-carbon steels tensile tested in the austenite phase field, higher strain rates lead to a gradual removal of the trough, and if the strain rate is sufficiently high, ductility will remain excellent at all temperatures. Here, GBS is dominating the fracture behaviour, i.e., creep conditions apply giving brittle intergranular failure at low strain rates. In contrast, in the absence of creep, normal ductile transgranular failure

occurs, which is inclusion- and dislocation-density-controlled, and lower strain rates will lead to better ductility.

At room temperature, most failures in tensile tests are transgranular ductile, in which case increasing the strain rate will rapidly increase the dislocation density, leading to early failure. In contrast, increasing the strain rate at elevated temperatures when creep conditions apply will generally give less time for grain boundary sliding and will thus improve ductility.

At the higher temperatures, DRX is most effective in restoring hot ductility, as it is continuous in removing dislocations and is particularly beneficial if the new recrystallised grains are finer. Recovery, in contrast, is dependent on the balance between the rate at which dislocations are accumulated and their rate of removal [12,13]. Hence, increasing the strain rate will have a negative effect on hot ductility when recovery is the main means of improving the ductility, and it is not sufficient to keep pace with the dislocations being created through deformation. The stacking fault energy (SFE) is a good indicator of whether recovery is more likely to occur, rather than DRX, as this controls cross-slip. If the SFE is low, the partial dislocations are well separated and cross-slip is difficult, favouring recrystallisation. If the SFE is high, the dislocations are close to each other, favouring cross-slip and recovery.

A table of SFEs [76] for a selection of common fcc metals and alloys at room temperature is given in Table 1 and shows the big difference between aluminium (180 mJm^{-2}) and austenitic stainless steel (20 mJm^{-2}) [76]. Bcc metals do not generally have stacking faults, being short of close-packed planes, and to achieve a stacking fault requires a very high SFE [77] such that recovery is favoured rather than GBS. Austenitic stainless steel can recrystallise more easily than ferritic, and the restoration of good ductility is often dramatic when DRX is possible. Thus, although Al has a high SFE (i.e., 180 mJm^{-2}), alloying reduces the SFE and Mg is particularly good at this; a 5% mass Mg addition results in the SFE falling to 20 mJm^{-2} , similar to that of stainless steel, and so will recrystallise and recover relatively easily (see Figure 17). Bcc alloys including iron have a high SFE and, hence, find recovery easier than DRX [12,13], and ductility improvements are generally lower. However, recovery is still very important and McQueen and Blum [13] showed that DRV can be a sufficient restoration mechanism in high-temperature deformation to provide a steady-state substructure in both Al alloys and α -Fe alloys.

Table 1. Experimental stacking fault energy (SFE) values of common metals and alloys at room temperature, data from [76].

Metal or Alloy	Stacking Fault Energy (mJm^{-2})
Al	180
Ni	75
Cu	75
Brass	25
Austenitic stainless steel	20
Al-5% Mg	20, Ref. [78]

The stacking fault energy for an Al-4.5% Cu alloy is even lower than the Al-5% Mg alloy [79], so that DRX is probably responsible for the improvement in ductility at the high-temperature end of the trough; Figure 11. The difference in strain rate behaviour between the Al-Cu alloy and the Al-Mg alloy may suggest that there is a liquid film at the boundaries in the Al-Mg alloys causing the embrittlement so that sliding becomes very easy. In the case of the Al-Cu alloys, the more normal behaviour for an fcc alloy is shown, with ductility improving with increase in strain rate.

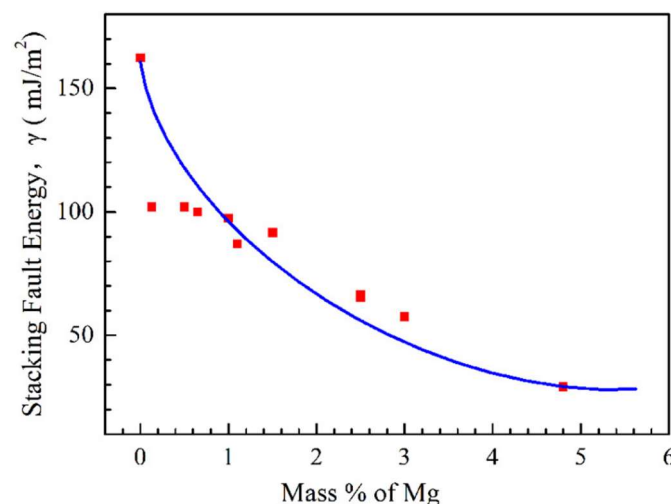


Figure 17. Influence of stacking fault energy as the amount of Mg increases in aluminium, data from [79–81].

In the case of creep, the hot ductility is controlled by what is happening at the grain boundaries rather than in the matrix. At low strain rates, if the temperature is sufficiently high, creep conditions occur and the failure is intergranular, not transgranular. Thus, it is probable that intergranular low-ductility failures can occur in all metals and alloys if the strain rate is slow enough and the temperature high enough to encourage creep.

It might be expected that when creep conditions apply (i.e., elevated temperatures and low strain rates), GBS leading to low-ductility intergranular failure would be the main form of intergranular failure, but this is not always so, because other forms of intergranular failure compete. In Al alloys, it is either low-melting compounds at the boundary or a weakening of the bonding by segregation of atoms to the boundary that can either weaken or strengthen the bonding there. Industrially, when Al-Mg alloys are hot rolled, this being one of the main processing routes, edge cracking can occur, so the ductility at high strain rates is the most relevant, and creep conditions, although still important, are not generally controlling the ductility. Furthermore, even if continuous casting is used to cast Al alloys, it does not usually incorporate the slow strain rate of an unbending operation.

Once creep conditions are present, the condition of the boundary becomes very important, and an increase in the volume fraction of the precipitated particles there and a reduction in the spacing between particles will encourage crack growth. Not only this, but the bonding at the boundaries and, hence, the strength of the boundary has also been shown to be sensitive to the atoms segregating there [70,72,82–89].

Gittins and Tegart [90] first pointed out for steels that there is big difference in fracture behaviour when the conditions change from hot working to creep. For hot working, fractures are generally transgranular with relatively good ductility, whereas for creep conditions, failure is intergranular and ductility can be very poor. Generally, GBS has occurred at these elevated temperatures even when the final fracture appearance does not readily show this. Thus, it would be expected that the temperature range in which ductility can be poor will be related to the melting point, as for creep. Creep normally manifests itself when the temperature (T) > 0.3 – 0.4 (T_m), where T_m is the melting point in °C [91]. Hence for steel, copper, aluminium, and nickel, the ratios are 0.6, with the centre of the hot-ductility troughs being at ~900, 700, 250, and 400 °C, respectively, as noted in Table 2, with the data being taken from the literature [11,27,34,35,51,56,60]. Although Al alloys can have a hot-ductility trough in the intermediate-temperature region, it is most likely that when failure occurs on tensile testing these alloys in the temperature range of the trough, it is due to one of the following: the weakening of the cohesive strength of the boundaries, the formation of liquid films, or oxygen infiltration to the grain surfaces, rather than creep cavitation.

Table 2. The relationship between melting point and centre position of the intermediate-temperature embrittlement zone on the hot-ductility curves taken from the figures shown in this review.

Metal or Alloy	Melting Point (T_m) °C	Temp. Centre Hot-Ductility Trough °C	Ratio: Temperature at the Centre of Hot-Ductility Trough HD/ T_m
Steel	1540	900	0.6
Nickel	1455	800	0.5
Copper	1085	700	0.6
Cast iron	1050	350–500	0.4
Aluminium	660	250	0.4

9. Importance of Segregation of Atoms and Ionic Bonding to the Cohesive Strength of Grain Boundaries

In the case of the segregation, it has relevant importance to the hot ductility due to its effect on the cohesive strength of grain boundaries. It is often suggested that the segregation of atoms to the grain boundaries at room temperature dictates the properties of metals such as strength, ductility and impact behaviour, corrosion, and weldability, particularly so for steel [50,51,55,87]. There is also a movement to use segregation to the boundaries as a means of designing alloys (DEA). This has arisen through the developments that have been made for understanding the crystallography of the boundary [83,92–95] as well as the introduction of atom probe microscopy, which has enabled segregation maps to be made of the grain boundary segregation across the boundary [67,93]. However, because grain boundary segregation normally involves atomic segregation, this makes it a difficult research field.

The trough is normally centred at a temperature about half the melting point of the alloy. However, although segregation is often proposed as the cause, proof of this is only just beginning to be found.

Generally, segregation can be related to the solubility of the solute in the matrix solvent; the smaller this is, the greater is the likelihood of segregation occurring [86,87]. Hence, impurities or small additions of elements, such as B or S, with very low solubility in solution in the matrix in C-Mn steels segregate to the boundaries. Once there, they can either weaken (S) or strengthen (B) the boundary. When strengthening occurs, it not only improves the strength of the alloy but also prevents intergranular failure. Although much is known about the beneficial or deleterious influence of these elements when segregation occurs, there is still a lack of understanding of the reasons for their powerful effect on properties, although headway is being made. It seems likely that in metals, the cohesion at the boundaries is mainly controlled by the electronic attraction between the positive metal ions and the sea of electrons surrounding them [87]. Messmer and Briant [87] proposed that electronegative impure atoms acquire electrons from surrounding metals and weaken grain boundary bonding, while electropositive impurity metal atoms transfer electrons to adjacent solvent metal atoms to enhance grain boundary bonding. The greater the number of free electrons, the greater is the bonding. When non-metallic elements such as P and S segregate, they reduce the pool of free electrons. When metallic solute elements, such as Na, segregate to the grain boundaries of Al alloys, they weaken the bonding by reducing the number of free electrons, with Al being trivalent and Na having a valency of one. The transition elements, Ce, La, Y, because they have many free electrons, also seem beneficial. Boron, because it is trivalent, is beneficial in steel (Fe has a valency of 2 or 3), and because it is an interstitial atom, packing presents no problems.

Huang et al. [96,97] have made considerable progress in understanding the relative influence of atomic size and electronic interaction on the strength of the grain boundaries in Cu. In these research papers, it is calculated that for the various elements they added to Cu, the solutes with a larger atomic radius segregated more easily to the grain boundaries, giving the most embrittlement. The electronic interactions between the Cu and the solute atoms played the biggest part in the strengthening of the bonding at room temperature,

and the d state electronic attractions between the transition metals and Cu could counteract the embrittlement effect caused by the size mismatch and significantly strengthen the bonding. Huang et al. [96,97] showed that B strengthened the boundaries by an increase in charge density at the boundaries, whilst S weakened the boundaries from a reduction in the charge density.

The changes in cohesive energy holding the boundary together have to be related to the changes in bonding, and these can now be measured using spatially resolved electron energy loss spectroscopy (EELS) [84].

Temper embrittlement in low-alloy steels is another area where grain boundary segregation is important, as there are many trace elements that can segregate and lower the cohesive strength of the prior austenite grain boundaries, leading to intergranular brittle failure after tempering in the range 400–600 °C [98–102]. In the case of temper embrittlement, it is the notch toughness that is being examined, and, as such, AES is a standard technique for examining the fracture surface and identifying and quantifying any segregation present when the failure mode is intergranular. Thus, although temper embrittlement is very different to hot ductility, much useful information can be gleaned from papers on the subject.

The common embrittling elements that are found are from groups IV and VI in the periodic table (e.g., Si, Ge, and Sn from group IV; P, As, and Sb from group VA; and S, Se, and Te from group VIA).

These elements in steel diffuse along the prior austenite grain boundaries, lowering the cohesive strength of the boundary. Yu and McMahon [98] examined the influence of Si and Mn on the temper embrittlement of a C martensitic stainless steel SS 420 (13% Cr, 0.25% C with 0.02% P), which is also very prone to this type of failure, with the segregation of P and Cr along the prior austenite boundaries causing the problem. Cr is found to enhance the detrimental effect of P [98]. Although the elements causing embrittlement on tempering are very often the same as those for hot ductility, this is not always the case (e.g., P improving the hot ductility in Al-Mg alloys).

Transgranular fracture is a ductile failure, and the ductility is dependent on the cleanliness of the metal or alloy and is generally inclusion-controlled, with the stress acting on the inclusions causing vacancies to be produced which join up to form cavities which link up to give failure across the matrix. This failure is normally associated with hot working when the stresses and the strain rate are high (i.e., 1 to 500 s^{−1}). Creep failure, in contrast, is intergranular and depends on the degree of grain boundary sliding that occurs. Here, strain rates are low: 10^{−4} to 10^{−10} s^{−1}. Thus, as the strain rate during the bending operation when steel is straightened is in the range 10^{−3} to 10^{−4} s^{−1} and the straightening temperature is 800–900 °C, creep conditions apply and ductility can be very poor, leading to cracking. When grain boundary sliding is most marked, as it is at elevated temperatures, the reduction in area values will be very low, much lower than given by ductile transgranular failure. When grain boundary sliding is not prevalent (i.e., too low a temperature or too high a strain rate) then failure will be transgranular and ductility will improve. Hence, the low-ductility intergranular failures at the base of the trough correspond to when creep conditions are applying. At the high-temperature end, creep conditions are prevented by dynamic recrystallization isolating the developing cracks from the grain boundaries or dynamic recovery preventing a build-up of dislocations. A simple model for this is shown in Figure 18, for how the depth and position of the trough is influenced by the critical strain for DRX, but this applies only to fcc metals and alloys.

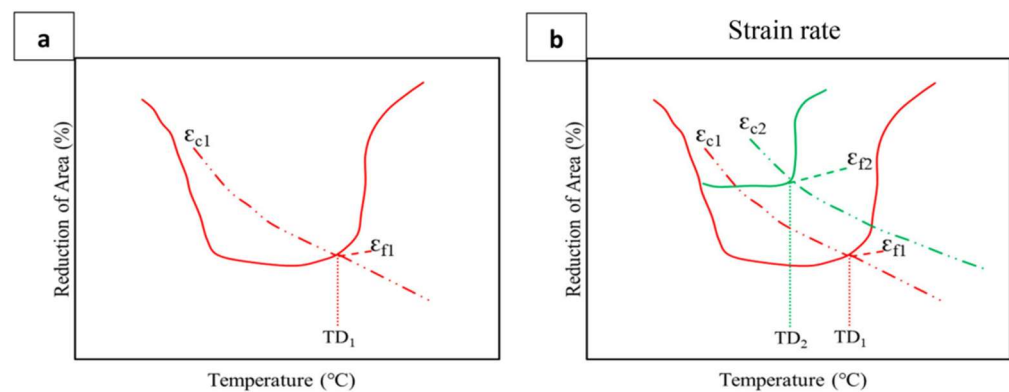


Figure 18. Schematic diagram showing (a) how the width of the ductility trough at the high-temperature side of the trough could be controlled by where the curve for ϵ_{c1} , the critical strain for DRX, intersects the curve for ϵ_{f1} , the fracture strain at TD_1 , giving the temperature for DRX; (b) how increasing the strain rate reduces the depth and width of this trough, where ϵ_{c1} , ϵ_{f1} and TD_1 refer to the lower strain rate, and ϵ_{c2} , ϵ_{f2} and TD_2 refer to the higher strain rate, reprint from [3], 2021, Taylor & Francis.

Two curves are proposed, as shown in Figure 18a: one of the fracture strain, ϵ_f , against temperature and the other for the critical strain for DRX, ϵ_c , against temperature, and where the curves intersect, this gives the temperature at which DRX occurs, TD_1 . The fracture strain is taken as the RA value at the base of the trough, and ϵ_c can be calculated as in Ref. [103]. Increasing the strain rate (see Figure 18b) will lead to a narrower and more ductile trough. The Ae_3 and Ar_3 temperatures will always give a good guidance as to the width of the trough, as they often span the entire temperature range in which the thin film of deformation-induced ferrite is formed.

Another important intergranular failure is segregation to the boundaries resulting in low-melting-point compounds. This occurs in steel with Cu and P segregation and Al-Mg alloys with Na. This leads to hot shortness in steel and intergranular brittle fracture in Al-Mg alloys. P is an unusual element as it can be either beneficial or detrimental to ductility. This may be because it is a metalloid and a very reactive element with a strong tendency to segregate to the grain boundaries. It has five valence electrons and can either donate or take valence electrons to make up a stable shell. Because P diffuses so rapidly in steels, it can often outpace other segregates, such as Nb or Mg, which can have a more detrimental influence on ductility [6]. However, too much segregation of P in the steel results in low-melting-point iron phosphate phases forming, resulting in almost zero ductility [20].

In Al alloys, intermediate intergranular embrittlement is a worry only in a few alloys in the industry, as their main processing routes are cold or hot rolling, where the strain rates are high, and extrusion, where creep conditions do not normally apply. Failures can still be low-ductility intergranular if segregation takes place, leading to the boundaries forming liquid films.

10. Summary and Conclusions

- (1) Low-ductility intergranular failures (intermediate-temperature embrittlement) can occur in both fcc and bcc alloys, but the causes are very diverse and, in many cases, not known with certainty because many of these explanations occur together and are synergistic.
- (2) In low- and medium-C steels, troughs can be caused by the thin film of ferrite, PFZs, segregation of deleterious elements to the boundaries influencing the bonding, and segregation to the boundaries leading to low-melting-point compounds. In other metals and alloys, the same origins apply, other than the presence of the ferrite film.

- (3) In steel and Ni alloys, creep failure is an important consideration as the unbending operation during continuous casting is so slow (10^{-3} – 10^{-4} s $^{-1}$) and the temperature range is within the creep temperature range. The austenite phase in steel, at temperatures in the range 750–950 °C, is particularly prone to this low ductility due to the low strain rate pertaining to the bending operation. This does not take place in hot rolling when the strain rate is much higher.
- (4) Hence, increasing the strain rate, refining the grain size, and coarsening of the precipitates will all lead to an improvement in ductility of steel, nickel, and copper alloys.
- (5) Of all the ways of improving hot ductility, refining the as-cast grain size is the most effective.
- (6) The depth of the trough is very much influenced in low–medium-C steel by the presence of the ferrite film or, more generally, when the film is absent by the precipitates at the grain boundaries and/or atoms which segregate to the boundaries and alter the bonding.
- (7) The improvement in ductility at the high-temperature end of the trough is due to DRX in the case of fcc metals with low SFE or recovery in fcc metals with high SFE and bcc metals.
- (8) In Al alloys, intermediate intergranular embrittlement is a worry only in a few alloys in industry, as the main processing routes are cold or hot rolling, where the strain rates are high, and extrusion, where creep conditions do not normally apply. Failures can still be low-ductility intergranular if segregation takes place, leading to the boundaries forming liquid films, hydrogen and oxygen infiltration, or substantial weakening of the cohesive strength of the boundaries by foreign atoms. Although the magnitude of the effect is very variable, refining the grain size will always benefit hot ductility.
- (9) The review highlights the importance of grain boundary segregation, both equilibrium and nonequilibrium segregation, in controlling hot ductility, and it is felt that this is an area which has considerable potential in not only improving hot ductility but the room-temperature properties of metals and alloys, and further research should be focused in this direction. Although our understanding of segregation is still limited, techniques are available to clarify our understanding. Using grain boundary segregation to improve properties is also likely to prove very cost-effective, as strengthening the boundaries rather than the matrix will require very little solute.

Funding: This research received no external funding.

Data Availability Statement: Not applicable.

Conflicts of Interest: The authors declare no conflicts of interest.

References

1. Mintz, B. The influence of composition on the hot ductility of steels and to the problem of transverse cracking. *ISIJ Int.* **1999**, *39*, 833–855. [CrossRef]
2. Mintz, B.; Crowther, D.N. Hot ductility of steels and its relationship to the problem of transverse cracking in continuous casting. *Int. Mater. Rev.* **2010**, *55*, 168–196. [CrossRef]
3. Mintz, B.; Qaban, A. Understanding the high temperature side of the hot ductility curve for steels. *Mater. Sci. Technol.* **2021**, *37*, 237–249. [CrossRef]
4. Zaitsev, A.; Arutyunyan, N.; Koldaev, A. Hot ductility, homogeneity of composition, structure and properties of high strength microalloyed steels: A critical review. *Metals* **2023**, *13*, 1066. [CrossRef]
5. Mintz, B.; Qaban, A. The influence of precipitation, high levels of Al, Si, P and a small B addition on the hot ductility of TWIP and TRIP assisted steels: A critical review. *Metals* **2022**, *12*, 502. [CrossRef]
6. Mintz, B.; Yue, S.; Jonas, J.J. Hot ductility of steels and its relationship to the problem of transverse cracking during continuous casting. *Int. Mater. Rev.* **1991**, *36*, 187–220. [CrossRef]
7. Melford, D.A. The influence of residual and trace elements on hot shortness and high temperature embrittlement. *Phil. Trans. R. Soc. Lond. A* **1980**, *295*, 89–103. Available online: <https://www.jstor.org/stable/36461> (accessed on 13 December 2023).
8. Perrot-Simonetta, M.T.; Kobylanski, A. Influence of trace elements on hot ductility of an ultra high purity invar alloy. *J. Phys. IV* **1995**, *5*, C7-323–C7-334. [CrossRef]

9. Cardoso, G.; Mintz, B.; Yue, S. Hot ductility of Al and Ti containing steels with and without cyclic temperature oscillations. *Ironmak. Steelmak.* **1995**, *22*, 365–377. Available online: <https://pascal-francis.inist.fr/vibad/index.php?action=getRecordDetail&idt=2928417> (accessed on 13 December 2023).
10. Ouchi, C.; Matsumoto, K. Hot ductility in Nb-bearing High-strength low-alloy steels. *Trans. ISIJ* **1982**, *22*, 181–189. [[CrossRef](#)]
11. Mintz, B.; Shaker, M.; Crowther, D.N. Hot ductility of an austenitic and a ferritic stainless steel. *Mater. Sci. Technol.* **1997**, *13*, 243–249. [[CrossRef](#)]
12. Sakai, T.; Jonas, J.J. Recovery and Recrystallisation in Encyclopedia of Materials Science and Technology, 2011.
13. McQueen, H.J.; Blum, W. Dynamic recovery: Sufficient mechanism in the hot deformation of Al (<99.99). *Mater. Sci. Eng. A* **2000**, *290*, 95–107. [[CrossRef](#)]
14. Liu, Z.; Yu, H.; Wang, K.; Xu, T. Nonequilibrium grain-boundary segregation mechanism of hot ductility loss for austenitic and ferritic stainless steels. *J. Mater. Res.* **2015**, *30*, 2117–2123. [[CrossRef](#)]
15. Peng, H.-B.; Chen, W.-Q.; Chen, L.C.; Guo, D. Effect of tin, copper and boron on the hot ductility of 20CrMnTi steel between 650 °C and 1100 °C. *High Temp. Mater. Proc.* **2015**, *34*, 19–26. [[CrossRef](#)]
16. Xu, T.; Zheng, L.; Wang, K.; Misra, R.D.K. Unified mechanism of intergranular embrittlement based on non-equilibrium grain boundary segregation. *Inter. Mater. Rev.* **2013**, *58*, 263–295. [[CrossRef](#)]
17. Kang, M.H.; Lee, J.S.; Koo, Y.M.; Kim, S.-J.; Heo, N.H. Correlation between MnS precipitation, sulfur segregation kinetics and hot ductility in C-Mn steel. *Metall. Mater. Trans. A* **2014**, *45*, 5295–5299. [[CrossRef](#)]
18. Laha, K.; Kyono, J.; Kishimoto, S.; Shinya, N. Beneficial effect of B segregation on creep cavitation in a type 347 austenitic stainless steel. *Scr. Mater.* **2005**, *52*, 675–678. [[CrossRef](#)]
19. Heo, N.H.; Shin, H.S.; Kim, S.-J. Role of power ratio on ductility-dip cracking of Ni-Cr-Fe weld. *Met. Mater. Int.* **2014**, *20*, 129–133. [[CrossRef](#)]
20. Mintz, B.; Cowley, A.; Talian, C.; Crowther, D.N.; Abushosha, R. Influence of P on the hot ductility of high C, Al, and Nb containing steels. *Mater. Sci. Technol.* **2003**, *19*, 184–188. [[CrossRef](#)]
21. Comineli, O.; Qaban, A.; Mintz, B. Influence of Cu and Ni on the hot ductility of low C steels with respect to the straightening operation when continuous casting. *Metals* **2022**, *12*, 1671. [[CrossRef](#)]
22. Jiang, X.; Chen, X.M.; Song, S.H.; Shangguan, Y.J. Phosphorus-induced hot ductility enhancement of 1Cr-0.5Mo low alloy steel. *Mater. Sci. Eng. A* **2013**, *574*, 46–53. [[CrossRef](#)]
23. Prasad, R. Influences of the formation of cast iron with nodular graphite using magnesium treatment processes. *Inter. Res. J. Eng. Technol.* **2022**, *9*, 489–493. Available online: <https://www.irjet.net/archives/V9/i5/IRJET-V9I594.pdf> (accessed on 13 December 2023).
24. Wright, R.N.; Farrell, T.R. Elevated temperature brittleness of ferritic ductile iron. *Trans. Am. Foundrymen's Soc.* **1985**, *93*, 853–866.
25. González-Martínez, R.; Sertucha, J.; Lacaze, J. The mechanism of intermediate temperature embrittlement of cast irons by magnesium. *Mater. Today Commun.* **2023**, *35*, 106128. [[CrossRef](#)]
26. Kobayashi, T.; Nishino, K.; Kimoto, J.; Awano, Y.; Hibino, Y.; Ueno, H. 673K embrittlement of ferritic spheroidal graphite cast iron by magnesium. *J. Jpn. Foundry Eng. Soc.* **1998**, *70*, 273–278.
27. Iwabuchi, Y.; Kobayashi, I. Suppression of elevated temperature brittleness in spheroidal graphite cast iron by increasing phosphorus content. *Key Eng. Mater.* **2011**, *457*, 428–432. [[CrossRef](#)]
28. Chen, S.F.; Lui, T.S.; Chen, L.H. The effect of phosphorus segregation on the intermediate-temperature embrittlement of ferritic, spheroidal graphite cast iron. *Metall. Mater. Trans. A* **1994**, *25*, 557–561. Available online: <https://link.springer.com/article/10.1007/BF02651597> (accessed on 13 December 2023). [[CrossRef](#)]
29. Yanagisawa, O.; Ishii, H.; Matsugi, K.; Hatayama, T. 673K embrittlement of ferritic spheroidal graphite cast iron with low residual magnesium content. *J. Jpn. Foundry Eng. Soc.* **2000**, *72*, 604–609. [[CrossRef](#)]
30. Yanisawa, O.; Lui, T.S.; Lin, H. Influence of structure on the 673 K embrittlement of ferritic ductile iron. *Trans. Jpn. Inst. Metals* **1983**, *24*, 858–867. [[CrossRef](#)]
31. Oikawa, H. Lattice diffusion in iron—A review. *Tetsu Hagané* **1982**, *68*, 1489–1497. [[CrossRef](#)] [[PubMed](#)]
32. Seah, M.P. Adsorption-induced interface decohesion. *Acta Metall.* **1980**, *28*, 955–962. [[CrossRef](#)]
33. Okada, H.; Kanno, M. Hot ductility of Al-Mg and Al-Mg-Y alloys impaired by trace sodium. *Scripta Mater.* **1997**, *37*, 781–786. [[CrossRef](#)]
34. Horikawa, K.; Kuramoto, S.; Kanno, M. High temperature embrittlement caused by traces of calcium or strontium in an Al-5.5mol%Mg alloy. *Scr. Mater.* **1998**, *37*, 861–866. [[CrossRef](#)]
35. Horikawa, K.; Kuramoto, S.; Kanno, M. Sources of a trace amount of sodium, and its effect on hot ductility of an Al-5 mass%Mg alloy. *Light Metals Rev.* **2000**, *7*, 18–23.
36. *Aluminum: Properties and Physical Metallurgy*; Hatch, J.E. (Ed.) American Society for Metals: Metals Park, OH, USA, 1984.
37. Turner, M.; Yeomans, S.; Ahmed, N. *Forum on "Aluminium in Ships"*; Aluminium Development Council (Manuka, Australia): Melbourne, Australia, 1995.
38. Sampath, D.; Moldenhaus, S.; Schipper, H.R.; Schrijvers, A.J.; Haszler, A.; Weber, G.; Mechsner, K.; Tack, L. Development of advanced ship building materials. In Proceedings of the 6th ICAA, Toyohashi, Japan, 5–10 July 1998; Japan Institute of Light Metals: Tokyo, Japan, 2009.

39. Godlewski, L.A.; Su, X.; Pollock, T.; Allison, J.E. The effect of aging on the relaxation of residual stress in cast aluminum. *Met. Mat. Trans. A* **2013**, *44*, 4809–4818. Available online: <https://link.springer.com/article/10.1007/s11661-013-1800-1> (accessed on 13 December 2023). [CrossRef]
40. Zhang, S.; Han, Q.; Liu, Z.-K. Fundamental understanding of Na-induced high temperature embrittlement in Al-Mg alloys. *Phil. Mag.* **2007**, *87*, 147–157. [CrossRef]
41. Deschamps, A.; Péron, S.; Bréchet, Y.; Ehrström, J.-C.; Poizat, L. High Temperature, high strain rate embrittlement of Al-Mg-Mn alloy: Evidence of cleavage of an fcc alloy. *Mater. Sci. Technol.* **2002**, *18*, 1085–1091. [CrossRef]
42. Ramsley, C.E.; Talbot, D.E.J. The embrittlement of aluminium-magnesium alloys by sodium. *J. Inst. Metals* **1959**, *88*, 150–158.
43. Scamans, G.M.; Alani, R.; Swann, P.R. Pre-exposure embrittlement and stress corrosion failure in Al-Zn-Mg alloys. *Corros. Sci.* **1976**, *16*, 443–459. [CrossRef]
44. Tuck, C.D.S. The embrittlement of Al-Zn-Mg and Al-Mg alloys by water vapor. *Metall. Trans. A* **1985**, *16*, 1503–1514. Available online: <https://link.springer.com/article/10.1007/BF02658682> (accessed on 13 December 2023). [CrossRef]
45. Horikawa, K.; Kuramoto, S.; Kanno, M. Intergranular fracture caused by trace impurities in an Al-5.5 mol% Mg alloy. *Acta Mater.* **2001**, *49*, 3981–3989. [CrossRef]
46. Kim, S.-J.; Ryu, K.M.; Oh, M.-S. Addition of cerium and yttrium to ferritic steel weld metal to improve hydrogen trapping efficiency. *Int. J. Miner. Metall. Mater.* **2017**, *24*, 415–422. Available online: <https://link.springer.com/article/10.1007/s12613-017-1422-5> (accessed on 13 December 2023). [CrossRef]
47. Talbot, D.E.J.; Granger, D.A. Effects of sodium and bismuth in aluminum-magnesium alloys. *JOM* **1995**, *47*, 44–46. Available online: <https://link.springer.com/article/10.1007/BF03221407> (accessed on 13 December 2023). [CrossRef]
48. Ueda, K.; Horikawa, K.; Kanno, M. Suppression of high temperature embrittlement of Al-5%Mg alloys containing a trace of sodium caused by antimony addition. *Scr. Mater.* **1997**, *37*, 1105–1110. [CrossRef]
49. Lynch, S.P. Comments on “Intergranular fracture caused by trace impurities in an Al-5.5 mol% Mg alloy. *Scr. Mater.* **2002**, *47*, 125–129. [CrossRef]
50. Suzuki, S.; Lejeck, P.; Hofmann, S. Effect of metallurgical factors on grain boundary segregation of solute atoms in iron. *Mater. Trans. JIM* **1999**, *40*, 463–473. [CrossRef]
51. Hammad, A.-H.M.; Ramadan, K.K. Mechanical properties of Al-Mg alloys at elevated temperatures. *Int. J. Mater. Res.* **1989**, *80*, 178–185. [CrossRef]
52. Lin, Y.C.; Dong, W.Y.; Zhu, X.H.; Wu, Q.; He, Y.J. Deformation behavior and precipitation features in a stretched Al-Cu alloy at intermediate temperatures. *Materials* **2020**, *13*, 2495. [CrossRef] [PubMed]
53. Liu, L.; Wu, Y.; Gong, H.; Li, S.; Ahmad, A.S. A physically based constitutive model and continuous dynamic recrystallisation behavior analysis of 2219 aluminum alloy during hot deformation process. *Materials* **2018**, *11*, 1443. [CrossRef] [PubMed]
54. Lui, L.; Wu, Y.; Gong, H.; Dong, F.; Ahmad, A.S. Modified kinetics model for describing continuous dynamic recrystallisation behavior of Al 2219 alloy during hot deformation process. *J. Alloys Compd.* **2020**, *817*, 153301. [CrossRef]
55. Otsuka, M.; Horiuchi, R. Ductility loss of Al-Mg alloys at high temperature. *J. Jpn. Inst. Met.* **1981**, *48*, 688–693. [CrossRef]
56. Gavin, S.A.; Billingham, J.; Chubb, J.P.; Hancock, P. Effect of trace impurities on hot ductility of as-cast cupronickel alloys. *Metals Technol.* **1978**, *5*, 397–401. [CrossRef]
57. Chubb, J.P.; Billingham, J. Effect of Ni on hot ductility of binary copper-nickel alloys. *Metals Technol.* **1978**, *5*, 100–103. [CrossRef]
58. White, C.L.; Schneibel, J.H.; Padgett, R.A. High temperature embrittlement of Ni and Ni-Cr alloys by trace elements. *Metall. Trans. A* **1983**, *14*, 595–610. Available online: <https://link.springer.com/article/10.1007/BF02643776> (accessed on 13 December 2023). [CrossRef]
59. Zheng, L.; Chellali, R.; Schlesiger, R.; Baither, D.; Schmitz, G. Intermediate temperature embrittlement in high-purity Ni and binary Ni(Bi) alloy. *Scr. Mater.* **2011**, *65*, 428–431. [CrossRef]
60. Hu, R.; Zhan, J.; Yang, C.; Du, J.; Luo, X.; Bi, Z.; Gan, B. Temperature effects on the deformation mechanisms in a Ni-Co-based superalloys. *Crystals* **2022**, *12*, 1409. [CrossRef]
61. Zheng, L.; Schmitz, G.; Meng, Y.; Chellali, R.; Schlesiger, R. Mechanism of Intermediate Temperature Embrittlement of Ni and Ni-based Superalloys. *Crit. Rev. Solid State Mater. Sci.* **2012**, *37*, 181–214. [CrossRef]
62. Lozinskiy, M.G.; Volkogon, G.M.; Pertsovskiy, N.Z. Investigation of the influence of zirconium additions on the ductility and deformation structure of nickel over wide temperature range. *Russ. Met.* **1967**, *5*, 65–72. Available online: https://jglobal.jst.go.jp/en/detail?JGLOBAL_ID=201602015193930837 (accessed on 13 December 2023).
63. Christien, F. Role of impurity sulphur in the ductility trough of austenitic iron-nickel alloys. *Materials* **2020**, *13*, 539. [CrossRef] [PubMed]
64. Bricknell, R.H.; Woodford, D.A. The embrittlement of nickel following high temperature air exposure. *Metal. Trans. A* **1981**, *12*, 425–433. Available online: <https://link.springer.com/article/10.1007/BF02648539> (accessed on 13 December 2023). [CrossRef]
65. Lu, X.; Ma, Y.; Wang, D. On the hydrogen embrittlement behavior of nickel-based alloys: Alloys 718 and 725. *Mater. Sci. Eng. A* **2020**, *792*, 139785. [CrossRef]
66. Iwasaki, H.; Kariya, R.; Mabuchi, M.; Tagata, T.; Higashi, K. Effects of temperature and strain rate on elongation at elevated temperature in Al - 4.5Mg alloy. *Mater. Trans.* **2001**, *42*, 1771–1776. [CrossRef]

67. Ebner, A.S.; Jakob, S.; Clemens, H.; Pippan, R.; Maier-Kiener, V.; He, S.; Ecker, W.; Scheiber, D.; Razumovskiy, V.I. Grain boundary segregation in Ni-base alloys: A combined atom probe tomography and first principles study. *Acta Mater.* **2021**, *221*, 117354. [CrossRef]
68. Saha, M. Grain boundary segregation in steels: Towards engineering the design of internal interfaces. *arXiv*, 2022; arXiv:arXiv:2022020096. [CrossRef]
69. Rajagopalan, M.; Tschopp, M.A.; Solanki, K.N. Grain boundary segregation of interstitial and substitutional impurity atoms in alpha-iron. *JOM* **2014**, *66*, 129–138. [CrossRef]
70. Lejcek, P. *Grain Boundary Segregation in Metals*; Springer: Berlin/Heidelberg, Germany, 2010.
71. Lejcek, P.; Sob, M.; Paidar, V. Interfacial segregation and grain boundary embrittlement: An overview and critical assessment of experimental data and calculated results. *Prog. Mater. Sci.* **2017**, *87*, 83–139. [CrossRef]
72. He, T.; Qi, Y.; Ji, Y.; Feng, M. Grain boundary segregation-induced strengthening-weakening transition and its ideal maximum strength in nanopolycrystalline FeNiCrCoCu high-entropy alloys. *Int. J. Mech. Sci.* **2023**, *238*, 107828. [CrossRef]
73. Han, L.; Xu, X.; Li, Z.; Liu, B.; Liu, C.T.; Liu, Y. A novel equiaxed eutectic high-entropy alloy with excellent mechanical properties at elevated temperatures. *Mater. Res. Lett.* **2020**, *8*, 373–382. [CrossRef]
74. Feng, C.; Wang, X.; Yang, L.; Guo, Y.; Wang, Y. High hardness and wear resistance in AlCrFeNiV high-entropy alloy induced by dual-phase body-centered cubic coupling effects. *Materials* **2022**, *15*, 6896. [CrossRef]
75. Mintz, B.; Lewis, J.; Jonas, J.J. Importance of deformation induced ferrite and factors which control its formation. *Mater. Sci. Technol.* **1997**, *13*, 379–388. [CrossRef]
76. Smallman, R.E.; Dillamore, I.L.; Dobson, P.S. The measurement of stacking fault energy. *J. Phys. Colloques* **1966**, *27*, C3-86–C3-93. Available online: <https://hal.science/jpa-00213120/document> (accessed on 13 December 2023). [CrossRef]
77. Ratanaphan, S.; Olmsted, D.L.; Bulatov, V.V.; Holm, E.A.; Rollett, A.D.; Rohrer, G.S. Grain boundary energies in body-centred cubic metals. *Acta Mater.* **2015**, *88*, 346–354. [CrossRef]
78. Lui, Y.; Liu, M.; Chen, X.; Cao, Y.; Roven, H.J.; Murashkin, M.; Valiev, R.Z.; Zhou, H. Effect of Mg on microstructure and mechanical properties of Al-Mg alloys produced by high pressure torsion. *Scr. Mater.* **2019**, *159*, 137–141. [CrossRef]
79. Muzyk, M.; Pakiel, Z.; Kurzydowski, K.J. Ab initio calculations of the generalized stacking fault energy in aluminum alloys. *Scr. Mater.* **2011**, *64*, 916–918. [CrossRef]
80. Morishige, T.; Hirata, T.; Uesugi, T.; Takigawa, Y.; Tsujikawa, M.; Higashi, K. Effect of Mg content on the minimum grain size of Al-Mg alloys obtained by friction stir processing. *Scr. Mater.* **2011**, *64*, 355–358. [CrossRef]
81. Schulthess, T.C.; Turchi, P.E.A.; Gonis, A.; Nieh, T.-G. Systematic study of stacking fault energies of random Al-based alloys. *Acta Mater.* **1998**, *46*, 2215–2221. [CrossRef]
82. Igwemezie, V.C.; Ugwuegbu, C.C.; Mark, U. Physical metallurgy of modern creep-resistant steel for steam power plants: Microstructure and phase transformations. *J. Metall.* **2016**, *2016*, 5468292. [CrossRef]
83. Li, Z.; Li, Z.; Tian, W. Strengthening effect of Nb on ferrite grain boundary in X70 pipeline steel. *Materials* **2021**, *14*, 61. [CrossRef] [PubMed]
84. Muller, D.A.; Subramanian, S.; Sass, S.L.; Silcox, J.; Batson, P.E. Local electronic structure and cohesion of grain boundaries in Ni₃Al. *MRS Online Proc. Lib.* **1994**, *364*, 743–748. [CrossRef]
85. Özerinç, S.; Tai, K.; Vo, N.Q.; Bellon, P.; Averbach, R.S.; King, W.P. Grain boundary doping strengthens nanocrystalline copper alloys. *Scr. Mater.* **2012**, *67*, 720–723. [CrossRef]
86. Briant, C.L. Solid solubility and grain boundary segregation. *Phil. Mag. Lett.* **1996**, *73*, 345–350. [CrossRef]
87. Messmer, R.P.; Briant, C.L. The role of chemical bonding in grain boundary embrittlement. *Acta Metall.* **1982**, *30*, 457–467. [CrossRef]
88. Nako, H.; Taniguchi, G.; Zhu, S.-Q.; Ringer, S.P. Influence of grain boundary segregation on temper embrittlement of Cr-Mo heat resistant steel weld metal and quantitative analysis of the amount of segregated atoms. In Proceedings of the 5th International Symposium on Steel Science (ISSS 2017), Kyoto, Japan, 13–16 November 2017. Available online: <https://www.isij.or.jp/publication/ISSS2017/data/iss2017-13.pdf> (accessed on 13 December 2023).
89. Briant, C.L.; Banerji, S.K. Intergranular failure in steel: The role of grain boundary composition. *Int. Met. Rev.* **1978**, *23*, 164–199. [CrossRef]
90. Gittins, A.; Tegart, W.J.M. From Creep to Working—Reflections on Fracture Modes. *Metals Forum.* **1981**, *4*, 57–62.
91. Roesler, J.; Harders, H.; Baeker, M. *Mechanical Behaviour of Engineering Materials: Metals, Ceramics and Composites*; Springer: Berlin, Germany, 2007. Available online: <https://link.springer.com/book/10.1007/978-3-540-73448-2> (accessed on 13 December 2023).
92. Olmsted, D.L.; Foiles, S.M.; Holm, E.A. Survey of computed grain boundary properties in face-centered cubic metals: I. Grain boundary energy. *Acta Mater.* **2009**, *57*, 3694–3703. [CrossRef]
93. Gault, B.; Breen, A.J.; Chang, Y.; He, J.; Jägle, E.A.; Kontis, P.; Kürnstener, P.; Da Silva, A.K.; Makineni, S.K.; Mouton, I.; et al. Interfaces and defect composition at the near-atomic scale through atom probe tomography investigations. *J. Mater. Res.* **2018**, *33*, 4018–4030. [CrossRef]
94. Pun, C.P.; Wang, W.; Khalajhedayati, A.; Schuler, T.D.; Trelewicz, J.R.; Rupert, T.J. Nanocrystalline Al-Mg with extreme strength due to grain boundary doping. *Mater. Sci. Eng. A* **2017**, *696*, 404–406. [CrossRef]
95. Da Rosa, G.; Maugis, P.; Portavoce, A.; Drillet, J.; Valle, N.; Lentzen, E.; Hoummada, K. Grain-boundary segregation of boron in high-strength steel studied by nano-SIMS and atom probe tomography. *Acta Mater.* **2020**, *182*, 226–234. [CrossRef]

96. Stoklosa, A.; Laskowska, B. Cohesion energy, metallic radius and bonding energy of electrons in the ionic core of metal atoms. *Arch. Metall. Mater.* **2005**, *50*, 783–801. Available online: <http://yadda.icm.edu.pl/baztech/element/bwmeta1.element.baztech-article-BW3-0017-0019> (accessed on 13 December 2023).
97. Huang, Z.; Wang, P.; Chen, F.; Shen, Q.; Zhang, L. Understanding solute effect on grain boundary strength based on atomic size and electronic attraction. *Sci. Rep.* **2020**, *10*, 16856. [[CrossRef](#)]
98. Huang, Z.; Chen, F.; Shen, Q.; Zhang, L.; Rupert, T.J. Combined effects of nonmetallic impurities and planned metallic dopants on grain boundary energy and strength. *Acta Mater.* **2019**, *166*, 113–125. [[CrossRef](#)]
99. Yu, J.; McMahon, C.J., Jr. The effects of composition and carbide precipitation on the temper embrittlement of 2.25 Cr-1 Mo steel: Part II. Effects of Mn and Si. *Metall. Trans. A* **1980**, *11*, 291–300. [[CrossRef](#)]
100. *Mechanical Metallurgy*; Dieter, G.E. (Ed.) McGraw-Hill Book Company: Singapore, 1988.
101. Mulford, R.A.; McMahon, C.J.; Pope, D.P.; Feng, H.C. Temper Embrittlement of Ni-Cr steels by phosphorus. *Met. Trans. A* **1976**, *7*, 1183–1195. [[CrossRef](#)]
102. Chandra, K.; Kain, V.; Srinivasan, N.; Samajdar, I.; Balasubrahmanian, A.K. Temper embrittlement and corrosion behaviour of martensitic stainless steel 420. *Adv. Mater. Res.* **2013**, *794*, 757–765. [[CrossRef](#)]
103. Mintz, B.; Abushosha, R.; Jonas, J.J. Influence of dynamic recrystallization on the tensile ductility of steels in the temperature range 700 to 1150 °C. *ISIJ Int.* **1992**, *32*, 241–249. [[CrossRef](#)]

Disclaimer/Publisher’s Note: The statements, opinions and data contained in all publications are solely those of the individual author(s) and contributor(s) and not of MDPI and/or the editor(s). MDPI and/or the editor(s) disclaim responsibility for any injury to people or property resulting from any ideas, methods, instructions or products referred to in the content.